Accessible and inaccessible quantum coherence in relativistic quantum systems

Saveetha Harikrishnan,[1, *] Segar Jambulingam,[2, †] Peter P. Rohde,[3, 4, ‡] and Chandrashekar Radhakrishnan[5, 1, §]

[1]*Centre for Quantum Science & Technology, Chennai Institute of Technology, Chennai 600069, India*
[2]*Department of Physics, Ramakrishna Mission Vivekananda College, Mylapore, Chennai 600 004, India*
[3]*Centre for Quantum Software & Information (UTS:QSI),*
University of Technology Sydney, Ultimo, NSW 2007, Australia
[4]*Hearne Institute for Theoretical Physics, Department of Physics & Astronomy,*
Louisiana State University, Baton Rouge LA, United States
[5]*Centre for Quantum Information, Communication and Computing,*
Indian Institute of Technology Madras, Chennai 600036, India

The quantum coherence of a multipartite system is investigated when some of the parties are moving with uniform acceleration and the analysis is carried out using the single mode approximation. Due to acceleration the quantum coherence is divided into two parts as accessible and inaccessible coherence and the entire analysis has been carried out in the single-mode approximation. First we investigate tripartite systems, considering both GHZ and W-states. We find that the quantum coherence of these states does not vanish in the limit of infinite acceleration, rather asymptoting to a non-zero value. These results hold for both single- and two-qubit acceleration. In the GHZ and W-states the coherence is distributed as correlations between the qubits and is known as global coherence. But quantum coherence can also exist due to the superposition within a qubit, the local coherence. To study the properties of local coherence we investigate separable state. The GHZ state, W-state and separable states contain only one type of coherence. Next we consider the $W\bar{W}$ and star states in which both local and global coherences coexist. We find that under uniform acceleration both local and global coherence show similar qualitative behaviour. Finally we derive analytic expressions for the quantum coherence of N-partite GHZ and W-states for $n < N$ accelerating qubits. We find that the quantum coherence of a multipartite GHZ state falls exponentially with the number of accelerated qubits, whereas for multipartite W-states the quantum coherence decreases only polynomially. We conclude that W-states are more robust to Unruh decoherence and discuss some potential applications in satellite-based quantum communication and black hole physics.

I. INTRODUCTION

Entanglement is a widely studied quantum resource with applications in quantum computing [1], quantum algorithms [2–4], metrology [5], teleportation [6, 7], and cryptography [8, 9]. In recent times, it has become more apparent that there are several other quantum properties such as non-locality [10], steering [11], discord [12] and coherence [13], which can also be used as a resource. Based on their relative presence, it is known that there is a hierarchy among these different resources. Of all these resources, quantum coherence is more extensively present, even when the quantum system does not have steering, entanglement or discord. Hence an investigation of quantum coherence can provide more complete information about the 'quantumness' of physical systems. Consequently, several studies have been performed into quantum coherence with the aim to understand the fundamental quantum behaviour of systems. Some important investigations carried out so far are on the measurement of quantum coherence [13, 14], the formulation of resource theory of quantum coherence [15–18], the effect of external environments on coherence [19, 20] and finally applications of quantum coherence [21–23].

Investigations in quantum information theory are generally carried out in inertial reference frames. An extension to non-inertial reference frames has been discussed through several works [24–27]. In this context entanglement in non-inertial frames of reference has been an important area of research [28–30]. Initial works [31] in this direction considered a family of peaked Minkowski wave packets which admits only a single Unruh mode. Later on the entanglement of a general set of states has been discussed in a multimode setting [32, 33]. Though the multimode approximation is more generally valid, several studies are still carried out in the single mode approximation [34], due to the ease of obtaining a clear analytic expression. Another approach is also available in non-inertial scenario by considering Unruh-Dewitt detector model[35, 36]. Several interesting results have been obtained in the fields of black hole physics [31, 37–41], quantum error correction [42], relativistic quantum metrology [43–46], relativistic teleportation [47–50] and communication [51–54]. Similar studies on relativistic effects on quantum discord [55, 56] have also been performed. Recent experimental advances have increased the scope of

* saveethah@citchennai.net
† segar@rkmvc.ac.in
‡ dr.rohde@gmail.com; https://www.peterrohde.org
§ chandrashekar10@gmail.com

quantum technologies from applications in terrestrial situations [57–59] to satellite-based space level technologies [60–66]. Hence, we investigate quantum coherence under uniform acceleration since compared to entanglement or other resources it is more commonly found and can be measured more easily.

The effect of relativistic motion on quantum coherence has been studied in the following works [67–70]. In Ref. [67], the relativistic effects on the quantum coherence between a pair of Unruh-Dewitt detectors is studied. Here they find that compared to entanglement, quantum coherence is more robust to Unruh decoherence. A generalisation of this result to tripartite system was performed by [69]. Both these works consider a massless scalar field. The relativistic coherence of a system of Dirac fields was considered in [70]. In our work we consider the modes of a massless scalar field and measure the coherence between different modes as well as the coherence within a mode. Here we consider a uniformly accelerating system which can be described using a family of peaked Minkowski wave packets and consequently we work in the single mode setting. We estimate the information-theoretic change in the coherence of the system using the ℓ_1-norm of coherence. For a complete study of tripartite systems, we investigate both the SLOCC (Stochastic Local Operations & Classical Communication) class of states, namely the GHZ (Greenberger-Horne-Zeilinger) and W class of states. But these two states have only global coherence which arises due to correlation between qubits. For completeness sake, we investigate the relativistic effects on separable states with only local coherence, a type of quantum coherence arising due to superposition within qubits. We also look into two different tripartite states, namely the $W\bar{W}$ and star states in which both global and local coherence coexist.

The structure of the manuscript is as follows: In Sec. II we discuss the notion of relativity in the field of quantum information and also introduce the ℓ_1-norm of coherence which is used to measure coherence in our work. The SLOCC class of states is studied in detail in Sec. III with the GHZ class and W class forming two different subsections. The separable state and an introduction to the notions of local coherence and global coherence is described in Sec. IV. The tripartite systems with both local and global coherence are analysed in Sec. V. In Sec. VI we discuss certain applications related to satellite-based communication as well as black holes. Finally in Sec. VII we discuss our results.

II.   RELATIVITY & QUANTUM COHERENCE

To describe events independent of the inertial frame of reference, the combination of three space and one time dimension known as Minkowski space are used. For non-inertial reference frames we need to use the Rindler co-ordinates. The Minkowski and Rindler co-ordinates are related to each other via a Rindler transformation. For a
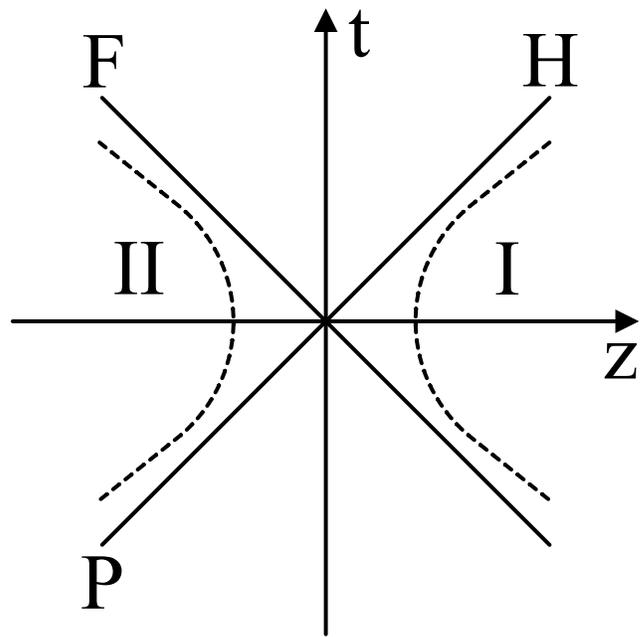
Figure 1: The (z, t) plane of the Minkowski co-ordinates is divided into four regions of the Rindler co-ordinates. The solid lines are the future (F) and past (P) event horizons and the dashed lines are the trajectories of the uniformly accelerated observers. Here H represents the horizon.

situation with one spatial and one time dimension (z, t), the Minkowski space-time is divided into four wedges as shown in Fig. 1. The regions F and P represent the future and the past light cones and the regions I and II are the two causally disconnected Rindler regions. The equations $|z| = t$ and $|z| = -t$ describe the future and past event horizons. For situations with one spatial and one time dimension (z, t), the world lines of uniformly accelerated observers in Minkowski co-ordinates correspond to a hyperbola. The two branches of the hyperbola constitute the regions I and II of the Rindler co-ordinates. The co-ordinates of the two regions are,

$$t = a^{-1}e^{a\xi}\sinh a\tau, z = a^{-1}e^{a\xi}\cosh a\tau; |z| < t,$$
$$t = -a^{-1}e^{a\xi}\sinh a\tau, z = a^{-1}e^{a\xi}\cosh a\tau; |z| > t. \quad (2.1)$$

where ξ is the space-like co-ordinate, τ is proper time, and a is acceleration.

Alice, Bob and Charlie each having monochromatic detector with their corresponding frequencies, ω_1, ω_2 and ω_3 of a free massless scalar field in a Minkowski space time. A maximally entangled GHZ state in the framework reads,

$$\frac{|0_{\omega_1}\rangle^{\mathcal{M}}|0_{\omega_2}\rangle^{\mathcal{M}}|0_{\omega_3}\rangle^{\mathcal{M}} + |1_{\omega_1}\rangle^{\mathcal{M}}|1_{\omega_2}\rangle^{\mathcal{M}}|1_{\omega_3}\rangle^{\mathcal{M}}}{\sqrt{2}}, \quad (2.2)$$

where $|0_{\omega_i}\rangle^{\mathcal{M}}$ ($|1_{\omega_i}\rangle^{\mathcal{M}}$) is the vacuum (single particle excitation) state of frequency ω_i in Minkowski space. Initially when all three parties are in inertial frames then $|0_{\omega_1}\rangle^{\mathcal{M}}$,

$|0_{\omega_2}\rangle^{\mathcal{M}}$ and $|0_{\omega_3}\rangle^{\mathcal{M}}$ are their respective ground states. Their excited states can be obtained by applying their corresponding Minkowski creation operators as follows,

$$|n_{\omega_i}\rangle^{\mathcal{M}} = \frac{(\hat{a}_{\omega_i}^{\dagger})^n}{\sqrt{n!}}|0_{\omega_i}\rangle^{\mathcal{M}}. \tag{2.3}$$

If Charlie starts moving with uniform acceleration the wavefunction becomes higly delocalized in space and the quantum state corresponding to the frequency ω_3 can be specified using Rindler or Unruh co-ordinates [32]. In both the Rindler and Unruh basis, the initial Minkowski space is divided into two regions which are casually disconnected from each other. Let Ω be the dimensionless Rindler frequency and the Unruh modes are also sharply peaked at the same frequency. Using an analytic continuation arguement it was shown [32] that Unruh mode is a purely positive frequency linear combinations of the Minkowski modes. But the definition of positive frequency in the Rindler mode differs from the positive frequency definition on the Minkowski mode. So we can relate the Minkowski and the Rindler modes via the Unruh modes. The field in each of these three bases are expanded as follows:

$$\begin{aligned}
\phi &= \int_0^{\infty} (a_{\omega,\mathcal{M}} u_{\omega,\mathcal{M}} + a_{\omega,\mathcal{M}}^{\dagger} u_{\omega,\mathcal{M}}^*)\, d\omega \\
&= \int_0^{\infty} (A_{\Omega,R} u_{\Omega,R} + A_{\Omega,R}^{\dagger} u_{\Omega,R}^* \\
&\quad + A_{\Omega,L} u_{\Omega,L} + A_{\Omega,L}^{\dagger} u_{\Omega,L}^*)\, d\Omega \\
&= \int_0^{\infty} (b_{\Omega,I} u_{\Omega,I} + b_{\Omega,I}^{\dagger} u_{\Omega,I}^* \\
&\quad + b_{\Omega,II} u_{\Omega,II} + b_{\Omega,II}^{\dagger} u_{\Omega,II}^*)\, d\Omega,
\end{aligned} \tag{2.4}$$

where $a_{\omega,\mathcal{M}}$ is the Minkowski annihilation operator and $A_{\Omega,R} \& A_{\Omega,L}$ are the Unruh annihilation operator for the right and left regions and $b_{\Omega,I} \& b_{\Omega,II}$ are the Rindler annihilation operators in $I \& II$ regions. The operators obey the bosonic commutation relations $[a_{\omega_1,\mathcal{M}}, a_{\omega_2,\mathcal{M}}^{\dagger}] = \delta_{\omega_1\omega_2}$, $[A_{\Omega_1,R}, A_{\Omega_2,R}^{\dagger}] = [A_{\Omega_1,L}, A_{\Omega_2,L}^{\dagger}] = \delta_{\Omega_1\Omega_2}$ and $[b_{\Omega_1,I}, b_{\Omega_2,I}^{\dagger}] = [b_{\Omega_1,II}, b_{\Omega_2,II}^{\dagger}] = \delta_{\Omega_1\Omega_2}$. For the Unruh mode, the commutator between operators in the R and L region vanish. Similarly the commutator between the operators in region I and II vanish. The creation and annihilation operators of the Minkowski and Unruh bases do not mix and hence we have $|0\rangle_M = |0\rangle_U = \prod_{\Omega} |0_{\Omega}\rangle_U$. But the state $|0\rangle_U$ does not coincide with the Rindler vacuum and we have

$$|0_{\Omega}\rangle_U = \sum_N \frac{\tanh^n r_{\Omega}}{\cosh r_{\Omega}} |n_{\Omega}\rangle_I |n_{\Omega}\rangle_{II}. \tag{2.5}$$

Here $|n_{\Omega}\rangle_I$ is the nth excited state of the Rindler I vacuum state $|0_{\Omega}\rangle_I$.

We consider a wave packet which is narrowly peaked in Ω and for this the Unruh and Rindler commutators read $[A_{\Omega,R}, A_{\Omega,R}^{\dagger}] = [A_{\Omega,L}, A_{\Omega,L}^{\dagger}] = 1$ and $[b_{\Omega,I}, b_{\Omega,I}^{\dagger}] = [b_{\Omega,II}, b_{\Omega,II}^{\dagger}] = 1$. Under these ideal conditions, the most general creation operator of a purely positive Minkowski frequency can be written as,

$$a_{\Omega,U}^{\dagger} = q_L A_{\Omega,L}^{\dagger} + q_R A_{\Omega,R}^{\dagger}. \tag{2.6}$$

Here the factors q_R and q_L are complex numbers with $|q_R|^2 + |q_L|^2 = 1$. Under these conditions we have

$$a_{\Omega,U}^{\dagger}|0_{\Omega}\rangle_U = \sum_{n=0}^{\infty} \frac{\tanh^n r_{\Omega}}{\cosh r_{\Omega}} \left(\frac{\sqrt{n+1}}{\cosh r_{\Omega}}\right)|\Phi_{\Omega}^n\rangle,$$
$$|\Phi_{\Omega}^n\rangle = q_L |n_{\Omega}\rangle_I |(n+1)_{\Omega}\rangle_{II} + q_R |(n+1)_{\Omega}\rangle_I |n_{\Omega}\rangle_{II}, \tag{2.7}$$

where, in general we consider $q_R = 1$ and $q_L = 0$. Let us consider a Minkowski smearing function which is a Gaussian in $\ln(\omega l)$,

$$f(\omega) = \left(\frac{\lambda}{\pi\omega^2}\right)^{1/4} \exp\left\{\frac{-1}{2}\lambda[\ln(\omega/\omega_0)]^2\right\}(\omega/\omega_0)^{-i\mu}, \tag{2.8}$$

When the uniformly accelerated particle has the above smearing function and has negligible overlap with the other states, then it is well approximated by a single Unruh frequency. Thus we use this monochromatic wave approximation in our investigation. Under this condition, the Minkowski and Rindler modes can be connected via the relations:

$$\begin{aligned}
\hat{a}_{\omega_3}^{\dagger} &= \hat{b}_{\Omega_3 I}^{\dagger} \cosh r - \hat{b}_{\Omega_3 II} \sinh r = \hat{S}_{\Omega_3} \hat{b}_{\Omega_3 I}^{\dagger} \hat{S}_{\Omega_3}^{\dagger} \\
\hat{a}_{\omega_3} &= \hat{b}_{\Omega_3 I} \cosh r - \hat{b}_{\Omega_3 II}^{\dagger} \sinh r = \hat{S}_{\Omega_3} \hat{b}_{\Omega_3 I} \hat{S}_{\Omega_3}^{\dagger},
\end{aligned} \tag{2.9}$$

where,

$$\hat{S}_{\Omega}(r) = \exp[r(\hat{b}_{\Omega I}^{\dagger} \hat{b}_{\Omega II}^{\dagger} - \hat{b}_{\Omega I} \hat{b}_{\Omega II})]. \tag{2.10}$$

Here the operator $(\hat{S})$ effecting the transformation from Minkowski co-ordinates to Rindler co-ordinates is structurally identical to the two mode squeezing operator,

$$\hat{S}(\zeta) = \exp(\zeta^* ab - \zeta a^{\dagger} b^{\dagger}), \tag{2.11}$$

in the quantum optics context. Hence for a non-inertial observer, the single mode Minkowski vacuum becomes a two mode squeezed state in the Rindler vaccum,

$$\begin{aligned}
|0_{\omega}\rangle^{\mathcal{M}} &= \hat{S}_{\Omega_3}(r)(|0\rangle_I \otimes |0\rangle_{II}) \\
&= \frac{1}{\cosh r} \sum_{n=0}^{\infty} \tanh^n r |n_{\Omega}\rangle_I |n_{\Omega}\rangle_{II}, \tag{2.12}
\end{aligned}$$

where $\cosh r = (1 - e^{-2\pi\Omega})^{-1/2}$ and $\Omega = |\omega|c/a$. The factors ω and c are the wave vector and velocity of light
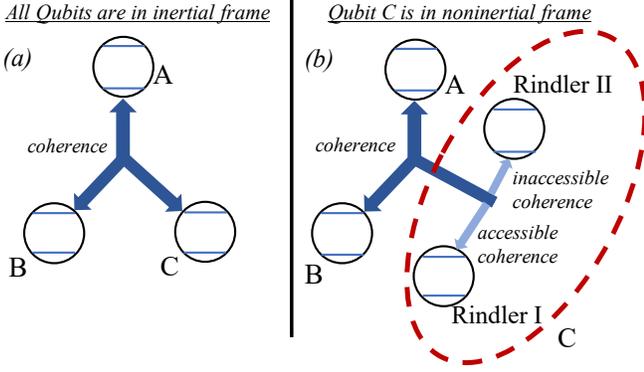
Figure 2: A schematic diagram of coherence in tripartite is shown where the circles labelled *A*, *B* and *C* represent the qubit and the blue arrow between them representing the coherence. Fig (a) contains the coherence in a tripartite system when all the qubits are in inertial frame. The part (b) contains the coherence in the tripartite system when qubit *C* is under acceleration. Here qubit *C* enclosed by the Red ellipse with dashed boundary line, is split into two Rindler modes I and II. Consequently the coherence shared by qubit *C* also is split into two parts. The coherence shared with *C* of Rindler mode I is the accessible coherence and the coherence shared with *C* of Rindler mode II is the inaccessible coherence. The lighter shades of blue for the accessible and inaccessible coherence represents their relative strength to the coherence initially present with *C* and shown in part (a).

respectively. Here $|n_\Omega\rangle_I$ and $|n_\Omega\rangle_{II}$ are the mode decom-

positions in Rindler regions I and region II respectively. For the single particle excitation state we have,

$$|1_\omega\rangle^{\mathcal{M}} = \hat{a}^\dagger_{\omega_3}|0_{\omega_3}\rangle^{\mathcal{M}} = \hat{S}_{\Omega_3}(r)\hat{b}^\dagger_{\Omega_3 I}(|0\rangle_I \otimes |0\rangle_{II})$$

$$= \frac{1}{\cosh^2 r}\sum_{n=0}^{\infty}\sqrt{n+1}\tanh^n r|(n+1)_\Omega\rangle_I|n_\Omega\rangle_{II}.$$

We observe that due to the squeezing behaviour of a non-inertial observer, a single Minkowski mode can be written as a superposition of two Rindler modes. Consequently there exists coherence between the two Rindler modes. Since these two modes are not causally connected, this coherence cannot be experimentally observed. Actually there is no new coherence created in the system.

To illustrate this let us consider a tripartite system with Alice and Bob at rest, and Charlie moving with constant acceleration. The coherence shared by Charlie with Alice and Bob is split into two parts. One part remains in Rindler mode I and can be experimentally observed, which we call the *accessible coherence*. The other part of the coherence which is shared with Rindler mode II cannot be measured, which we refer to as *inaccessible coherence*. This inaccessible coherence quantifies the decrease in coherence due to relativistic effects. A schematic diagram explaining the accessible and inaccessible coherence is shown in Fig. 2.

In a tripartite state when two qubits are accelerated the vacuum ($|000\rangle$) and excited ($|111\rangle$) states can be expressed as,

$$|000\rangle_{ABC} = |0\rangle \otimes |0\rangle \otimes |0\rangle$$

$$\xrightarrow{accl} |0_{\omega_1}\rangle \otimes [\hat{S}_{\Omega_2}(r_2)(|0_{\Omega_2}\rangle_I \otimes |0_{\Omega_2}\rangle_{II})] \otimes [\hat{S}_{\Omega_3}(r_1)(|0_{\Omega_3}\rangle_I \otimes |0_{\Omega_3}\rangle_{II})]$$

$$= |0\rangle \otimes \frac{1}{\cosh r_2}\left[\sum_{m=0}^{\infty}\tanh^m r_2|m\rangle_I|m\rangle_{II}\right] \otimes \left[\frac{1}{\cosh r_1}\sum_{n=0}^{\infty}\tanh^n r_1|n\rangle_I|n\rangle_{II}\right], \tag{2.13}$$

$$|111\rangle_{ABC} = |1\rangle \otimes |1\rangle \otimes |1\rangle$$

$$\xrightarrow{accl} |1_{\omega_1}\rangle \otimes [\hat{S}_{\Omega_2}(r_2)\hat{b}^\dagger_{\Omega_2 I}(|0_{\Omega_2}\rangle_I \otimes |0_{\Omega_2}\rangle_{II})] \otimes [\hat{S}_{\Omega_3}(r_1)\hat{b}^\dagger_{\Omega_3 I}(|0_{\Omega_3}\rangle_I \otimes |0_{\Omega_3}\rangle_{II})]$$

$$= |1\rangle \otimes \left[\frac{1}{\cosh^2 r_2}\sum_{m=0}^{\infty}\sqrt{m+1}\tanh^m r_2|m+1\rangle_I|m\rangle_{II}\right] \otimes \left[\frac{1}{\cosh^2 r_1}\sum_{n=0}^{\infty}\sqrt{n+1}\tanh^n r_1|n+1\rangle_I|n\rangle_{II}\right].$$

$$\tag{2.14}$$

The modes *I* and *II* correspond to the two causally disconnected regions in Rindler co-ordinates of Minkowski space. Hence mode *II* is physically inaccessible to Alice, Bob and Charlie and is partially traced out. For an inertial observer, a quantum system in Minkowski spacetime is independent of the nature of the observer. But when the observer is moving with constant acceleration, they perceive a thermal bath with temperature proportional to acceleration. This thermal bath is made up of

Rindler particles which are associated with the vacuum state of Minkowski space. Due to this thermal bath, the observer perceives decoherence of the quantum system, a phenomenon known as Unruh decoherence.

Quantum coherence is in general measured as the distance between the quantum state under consideration and the closest incoherent state in the same basis. Several measures of quantum coherence [13, 14, 71, 72] have been presented, but in the first work on quantum coherence by

Baumgratz, Cramer and Plenio [13] two measures were introduced corresponding to the entropic class and geometric class of measures. The relative entropy based measure of quantum coherence belongs to the entropic class, and the ℓ_1 norm of coherence to the geometric class. Here we use the ℓ_1-norm of quantum coherence, defined as,

$$C_{l_1}(\hat{\rho}, \hat{\rho}_d) = \|\hat{\rho} - \hat{\rho}_d\|_{l_1} = \sum_{i \neq j} |\hat{\rho}_{i,j}|, \qquad (2.15)$$

where $\hat{\rho}$ is a given density matrix and $\hat{\rho}_d$ is the associated decohered density matrix defined as,

$$\hat{\rho}_d = \sum_i \hat{\rho}_{i,i}|i\rangle\langle i|. \qquad (2.16)$$

We can observe that this is equivalent to the sum of the off-diagonal elements of the density matrix. Using interference fringes, the quantum coherence of a physical system can be measured using the robustness of coherence [73], a measure introduced in Ref. [74]. In Ref. [75] it was shown that for a pure state the robustness of coherence measure is equal to the ℓ_1-norm of coherence. Hence the ℓ_1-norm of coherence can be directly obtained from the interference fringes, providing a method to compare theoretical results with experimental data.

III. RELATIVISTIC EFFECTS IN THE SLOCC CLASS OF STATES

Based on the local operations and classical communication (LOCC), tripartite entangled quantum states can be divided into two distinct classes, namely the GHZ class and the W class. The entanglement distribution is different in these two class of states. In a GHZ state all the entanglement vanishes even with the loss of a single qubit whereas in a W-state a finite amount of entanglement is always present even when we loose a single qubit. The coherence of these class of states in inertial frames has been discussed in detail in Ref. [20]. We extend upon this by investigating the coherence when some of the qubits of the tripartite system are in a non-inertial reference frame. In particular, we probe the loss of coherence due to the acceleration of qubits.

III.1. GHZ class

A GHZ state is maximally entangled and so the loss of just a single qubit results in the complete loss of entanglement and coherence. The general form of a tripartite Greenberger-Horne-Zeilinger (GHZ) state is,

$$|\text{GHZ}\rangle_{ABC} = \cos\theta|000\rangle_{ABC} + \sin\theta|111\rangle_{ABC}, \qquad (3.1)$$

where $\theta \in [0, 2\pi)$ is a parameter generalizing the GHZ state via the bias between the two basis states. On accelerating qubit C its Minkowski modes are replaced with their corresponding Rindler modes and the tripartite states becomes,

$$|\text{GHZ}\rangle_{ABC} = \frac{1}{\cosh r} \sum_{n=0}^{\infty} \tanh^n r \left[\cos\theta|00\rangle|n\rangle_I|n\rangle_{II} + \frac{\sqrt{n+1}}{\cosh r} \sin\theta|11\rangle|n+1\rangle_I|n\rangle_{II} \right]. \qquad (3.2)$$

Here, $|00\rangle|n\rangle_I|n\rangle_{II}$ and $|11\rangle|n+1\rangle_I|n\rangle_{II}$ refer to the quantum state in which the Minkowski modes of the first two qubits are $|ab\rangle$ and the Rindler modes corresponding to the third qubit is as $|c\rangle_I|c\rangle_{II}$. We know that the modes from the Rindler I and II regions are not causally connected, so we can trace out the modes corresponding to Rindler region II and the density matrix of the state with Alice, Bob and Charlie reduces to,

$$\hat{\rho}_{\text{GHZ}} = \frac{1}{\cosh^2 r} \sum_{n=0}^{\infty} \tanh^{2n} r \left[\cos^2\theta|00n\rangle\langle 00n| + \cos\theta\sin\theta \frac{\sqrt{n+1}}{\cosh r} \left(|00n\rangle\langle 11n+1| + |11n+1\rangle\langle 00n| \right) \right.$$
$$\left. + \frac{n+1}{\cosh^2 r} \sin^2\theta|11n+1\rangle\langle 11n+1| \right]. \qquad (3.3)$$

The total coherence in the generalised GHZ state is calculated using the ℓ_1-norm measure of coherence. The
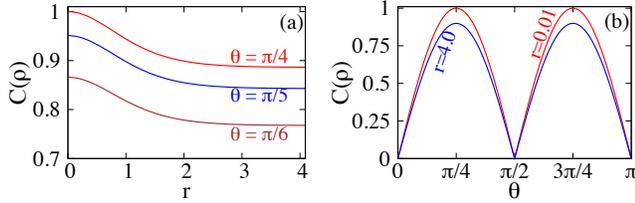
Figure 3: The variation of coherence in a non-inertial frame of reference is studied for a GHZ state under the variation of (a) the acceleration parameter r and (b) the generalisation parameter θ.

sum of the off-diagonal elements of Eq. (3.3) is

$$C(\hat{\rho}) = \frac{2\sin\theta\cos\theta}{\cosh^3 r}\sum_{n=0}^{\infty}\sqrt{n+1}\tanh^{2n} r. \qquad (3.4)$$

Using the trigonometric identities,

$$\sum_{n=0}^{\infty}\tanh^{2n} r = \cosh^2 r,$$

$$\sum_{n=0}^{\infty}(n+1)\tanh^{2n} r = \cosh^4 r, \qquad (3.5)$$

and the polylogarithm function

$$\mathrm{Li}_{-1/2}(z) = \sum_{n=0}^{\infty}\sqrt{n+1}(\tanh^2 r)^{n+1}, \qquad (3.6)$$

where the polylogarithm function is defined as

$$\mathrm{Li}_n(z) \equiv \sum_{k=1}^{\infty}\frac{z^k}{k^n} = \frac{z}{1^n} + \frac{z^2}{2^n} + \frac{z^3}{3^n} + \cdots, \qquad (3.7)$$

the total coherence of a GHZ state when one of the qubits is in a non-inertial frame can be expressed as,

$$C(\hat{\rho}) = 2\sin\theta\cos\theta\frac{\mathrm{Li}_{-1/2}(\tanh^2 r)}{\sinh^2 r\,\cosh r}. \qquad (3.8)$$

When Charlie's qubit is not accelerated (i.e the $r \to 0$ limit) the corresponding quantum coherence is,

$$C(\hat{\rho}) = 2\cos\theta\sin\theta. \qquad (3.9)$$

The variation of quantum coherence as a function of the acceleration parameter r is shown in Fig. 3(a) for different θ values. From the plot for any given value of θ we notice that quantum coherence has a maximum value when $r = 0$, corresponding to the situation where Charlie's qubit has not yet been accelerated. The coherence then decreases with increase in r and saturates to a finite value. The decrease in coherence due to uniform acceleration is because some part of it becomes inaccessible as it lies in a causally disconnected region. The saturation value depends on the value of coherence in the inertial frame ($r = 0$). Hence, higher the value of the coherence in the inertial frame, the higher the saturation value of coherence in the non-inertial frame.

In Fig. 3(b), we study the change of the quantum coherence as a function of the generalisation parameter θ for different values of the acceleration parameter r. The coherence is maximum at $\theta = (2n+1)\pi/4$ where $n \in \mathbb{Z}$ and is zero at $\theta = n\pi/2$, but the maximum value depends on the value of r.

To study the situation, when more than one party is under acceleration, we consider the setting where both Bob's and Charlie's qubits are being accelerated. The quantum state when two qubits are accelerated is,

$$
\begin{aligned}
|\mathrm{GHZ}\rangle = \frac{1}{\cosh r_1}\frac{1}{\cosh r_2}\sum_{n,m=0}^{\infty}\tanh^n r_1\tanh^m r_2\Bigg[& \cos\theta|0\rangle|m\rangle_I|m\rangle_{II}|n\rangle_I|n\rangle_{II} \\
+ \frac{\sqrt{m+1}}{\cosh r_2}\frac{\sqrt{n+1}}{\cosh r_1}\sin\theta \times |1\rangle|m+1\rangle_I|m\rangle_{II}|n+1\rangle_I|n\rangle_{II}\Bigg], & \qquad (3.10)
\end{aligned}
$$

where the pairs (r_2, m) and (r_1, n) are the acceleration parameter and mode corresponding to Bob's and Char-

lie's qubits respectively. To construct the density matrix we first trace out the contributions from the causally disconnected Rindler II mode,

$$\hat{\rho} = \frac{1}{\cosh^2 r_1 \cosh^2 r_2} \sum_{n=0}^{\infty} \sum_{m=0}^{\infty} \tanh^{2n} r_1 \tanh^{2m} r_2 \left[\cos^2 \theta |0\rangle|m\rangle|n\rangle\langle 0|\langle m|\langle n| + \frac{\sqrt{m+1}\sqrt{n+1}}{\cosh r_1 \cosh r_2} \cos \theta \sin \theta \right.$$

$$\left(|0\rangle|m\rangle|n\rangle\langle 1|\langle m+1|\langle n+1| + |1\rangle|m+1\rangle|n+1\rangle\langle 0|\langle m|\langle n| \right) + \frac{(m+1)(n+1)}{\cosh^2 r_1 \cosh^2 r_2} \sin^2 \theta$$

$$\left. |1\rangle|m+1\rangle|n+1\rangle\langle 1|\langle m+1|\langle n+1| \right], \tag{3.11}$$
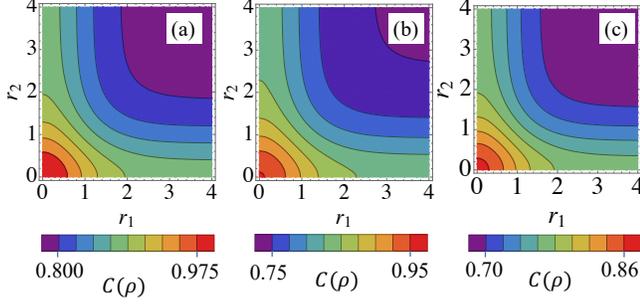
Figure 4: The variation of quantum coherence of GHZ state with both r_1 and r_2 is shown for (a) $\theta = \pi/4$, (b) $\theta = \pi/5$ and (c) $\theta = \pi/6$ respectively.

From the density matrix in Eq. (3.11) and using the ℓ_1-norm measure we can determine the total quantum coherence of the GHZ state when both Bob's and Charlie's qubits are accelerated,

$$C(\hat{\rho}) = 2\sin\theta\cos\theta \frac{Li_{-1/2}(\tanh^2 r_1)}{\sinh^2 r_1 \cosh r_1} \frac{Li_{-1/2}(\tanh^2 r_2)}{\sinh^2 r_2 \cosh r_2}, \tag{3.12}$$

where we find to be a product of two polylogarithm functions one each corresponding to Bob's and Charlie's qubits. If Bob and Charlie have the same acceleration, which would translate to $r_1 = r_2 = r$, the coherence would then be,

$$C(\hat{\rho}) = 2\sin\theta\cos\theta \left[\frac{Li_{-1/2}(\tanh^2 r)}{\sinh^2 r \cosh r} \right]^2. \tag{3.13}$$

The variation of quantum coherence with the parameters r_1 and r_2 corresponding to Bob's and Charlie's acceleration is shown through the contour plots in Fig. 4. The contour plots Fig. 4(a), 4(b) and 4(c) correspond to θ of $\pi/4$, $\pi/5$ and $\pi/6$ respectively. We find that with the increase in r_1 and r_2, the coherence decreases and saturates to a finite value. The maximal value and saturation value of coherence are dependent on the value of θ the parameter generalizing the GHZ state.

In literature, the most commonly discussed GHZ state is $(|000\rangle + |111\rangle)/\sqrt{2}$, corresponding to the generalised GHZ state with $\theta = \pi/4$, which has quantum coherence,

$$C(\hat{\rho}) = \frac{Li_{-1/2}(\tanh^2 r)}{\sinh^2 r \cosh r},$$

$$C(\hat{\rho}) = \frac{Li_{-1/2}(\tanh^2 r_1)}{\sinh^2 r_1 \cosh r_1} \frac{Li_{-1/2}(\tanh^2 r_2)}{\sinh^2 r_2 \cosh r_2}. \tag{3.14}$$

Finally we note that the two qubit reduced density matrices corresponding to the GHZ state are diagonal in nature and hence are incoherent. Thus all the coherences in the GHZ state are genuinely multipartite in nature and the loss of even one qubit removes all the coherence in the system.

In Ref. [31], the authors considered a two qubit system of which one qubit is moving with a constant acceleration. The entanglement of the bipartite system vanished in the infinite acceleration limit. It is well known that entanglement is just one of the different types of quantum correlations. Out of the different quantifiers of quantum correlations, quantum discord measures the total quantum correlations in the system. A study of quantum discord in relativistic system [55] show that total quantum correlations does not vanish in the infinite acceleration limit. Hence a bipartite system in the infinite acceleration limit has quantum correlations beyond the entanglement type. An investigation on accelerating tripartite systems was carried out in Ref. [76], where the GHZ and W-states were characterised using the π-tangle measure of entanglement. The entanglement of the tripartite system did not go to zero in the infinite acceleration limit, rather it showed a decrease initially and then attained a saturation value. This is in stark contrast to the behaviour of the bipartite entanglement. In Ref. [76] it was suggested that the incomplete definition of π-tangle could be the reason as to why the tripartite entanglement shows a different qualitative behaviour when compared to the bipartite entanglement as measured in Ref. [31]. Through the present work we observe that the quantum coherence of the GHZ state is qualitatively similar to the change in its tripartite entanglement. But here the saturation is due to the non-vanishing behaviour of local quantum correlations. However for quantum coherence, the ℓ_1-norm measures the entire quantum coherence and the saturation value is a physical feature of the system. In the case of entanglement, the saturation value may not be an actual physical feature since π-tangle is inadequate to measure entanglement.
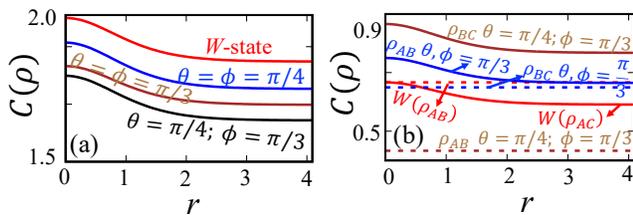
Figure 5: The variation of quantum coherence as a function of r for fixed values of θ and ϕ is given for (a) the tripartite generalized W-state and (b) the two qubit reduced systems ρ_{AB}, ρ_{BC} and ρ_{AC}. Here the notation $W(\rho_{AB})$ means the reduced state ρ_{AB} corresponding to the symmetric W-state.

Next we can consider the three qubit GHZ state given in Eq. (2.2) in which two qubits are under uniform acceleration. The GHZ state can be rewritten as $(|\mathbf{0}\mathbf{0}\rangle + |\mathbf{1}\mathbf{1}\rangle)/\sqrt{2}$, where $|\mathbf{0}\rangle = |00\rangle$ and $|\mathbf{1}\rangle = |11\rangle$ are redundantly-encoded logical qubits. Since the GHZ state can be written in terms of the Bell state, we would expect the coherences of both these states to be equal. But the coherence of the GHZ state when the logical qubit is accelerated is,

$$C_{\ell_1} = [Li_{-1/2}(\tanh^2 r)/(\sinh^2 r \cosh r)]^2, \qquad (3.15)$$

which implies that $C(|\psi_{Bell}\rangle) \neq C(|\psi_{GHZ}\rangle)$ an relativistic system. This is because in the GHZ state, the logical non-inertial qubit is bigger than the regular qubit considered in the Bell state. So, we find that the quantum coherence coupled with uniform acceleration helps in distinguishing between Bell states and GHZ states.

III.2. W class

The W-states exhibit non-maximal multipartite entanglement which is not locally equivalent to GHZ-type entanglement, and may therefore be considered a distinct entanglement class. Unlike GHZ states, W-states with large numbers of qubits are highly robust against qubit loss. The generalised form of the tripartite W-state is,

$$|W\rangle_g = \sin\theta\cos\phi|100\rangle + \sin\theta\sin\phi|010\rangle + \cos\theta|001\rangle, \qquad (3.16)$$

where $\theta = [0, \pi]$ and $\phi = [0, 2\pi)$ are the parameters generalising the W-state.

First let us consider the situation when only one qubit is in a non-inertial frame of reference. Towards this end, we consider the situation when Charlie's qubit is in a non-inertial frame while Alice and Bob's qubits are in an inertial frame. Naturally the Minkowski modes of Charlie's qubit are replaced by their corresponding Rindler modes. It is well known that the Minkowski region can be divided into two causally disconnected Rindler modes. So, we trace out the second Rindler region from the quantum state, since it is inaccessible for measuerment. The total

quantum coherence is then measured using the ℓ_1-norm of coherence,

$$C(\hat{\rho}) = 2\sin\theta\cos\theta(\sin\phi + \cos\phi)\frac{Li_{-1/2}(\tanh^2 r)}{\sinh^2 r \cosh r}$$
$$+ 2\sin^2\theta\sin\phi\cos\phi . \qquad (3.17)$$

To understand the relativistic effects on a quantum state with bipartite distribution, we compute the reduced density matrices corresponding to the W-state. Here, we can trace out either Alice or Bob's qubit and the quantum coherence corresponding to the reduced state is,

$$C(\hat{\rho}_{BC}) = C(\hat{\rho}_{AC}) = 2\sin\theta\cos\theta\sin\phi\frac{Li_{-1/2}(\tanh^2 r)}{\sinh^2 r \cosh r}. \qquad (3.18)$$

The reduced density matrix obtained after tracing out Charlie's qubit does not have any effects of non-inertial nature and the coherence of the joint state of Alice and Bob is,

$$C(\hat{\rho}_{AB}) = 2\sin^2\theta\sin\phi\cos\phi, \qquad (3.19)$$

which is the expected standard result. The most common form the three qubit W-state is the tripartite state of the form $|W\rangle = \frac{1}{\sqrt{3}}(|001\rangle + |010\rangle + |100\rangle)$, and of all the generalised W-states it has the maximum amount of coherence and entanglement. Also the total coherence and entanglement are distributed in a symmetric manner. The quantum coherence of a tripartite system when Charlie's qubit is accelerated is ,

$$C(\hat{\rho}) = \frac{4\,Li_{-1/2}(\tanh^2 r)}{3\cosh r\,\sinh^2 r} + \frac{2}{3}. \qquad (3.20)$$

In the $r \to 0$ limit (inertial limit), it reduces to the standard value of $C(\hat{\rho}) = 2$. The change in coherence of the tripartite generalised W-state is given as a function of the acceleration parameter r for different values of θ and ϕ in Fig. 5(a). From the plots we notice that the quantum coherence is initially maximum at $r = 0$ and then it decreases and reaches a saturation value at large values of r. The decrease in coherence is due to the bifurcation of the Minkowski mode into two Rindler modes, of which one is disconnected from the rest of the system. Any coherence due to this mode is inaccessible to measurements. The saturation value is the amount of accessible coherence which can never be lost to relativistic motion. The maximal value and saturation value are dependent on the generalisation parameter. The $|W\rangle = \frac{1}{\sqrt{3}}(|001\rangle + |010\rangle + |100\rangle)$ state has the maximal coherence at $r = 0$ and also has the maximal saturation value. The quantum coherence of the reduced density matrices of the generalised W-state is shown in Fig. 5(b). The quantum coherence of the reduced state $\hat{\rho}_{AB}$ is a constant since the accelerated qubit C has already been traced out. In the case of $\hat{\rho}_{BC}$ we find that the coherence is maximal at $r = 0$ and saturates to a finite value at large accelerations. The curve represents

(a)

$$0.2 \quad C(\rho) \quad 1.8$$

(b)

$$0.2 \quad C(\rho) \quad 1.8$$
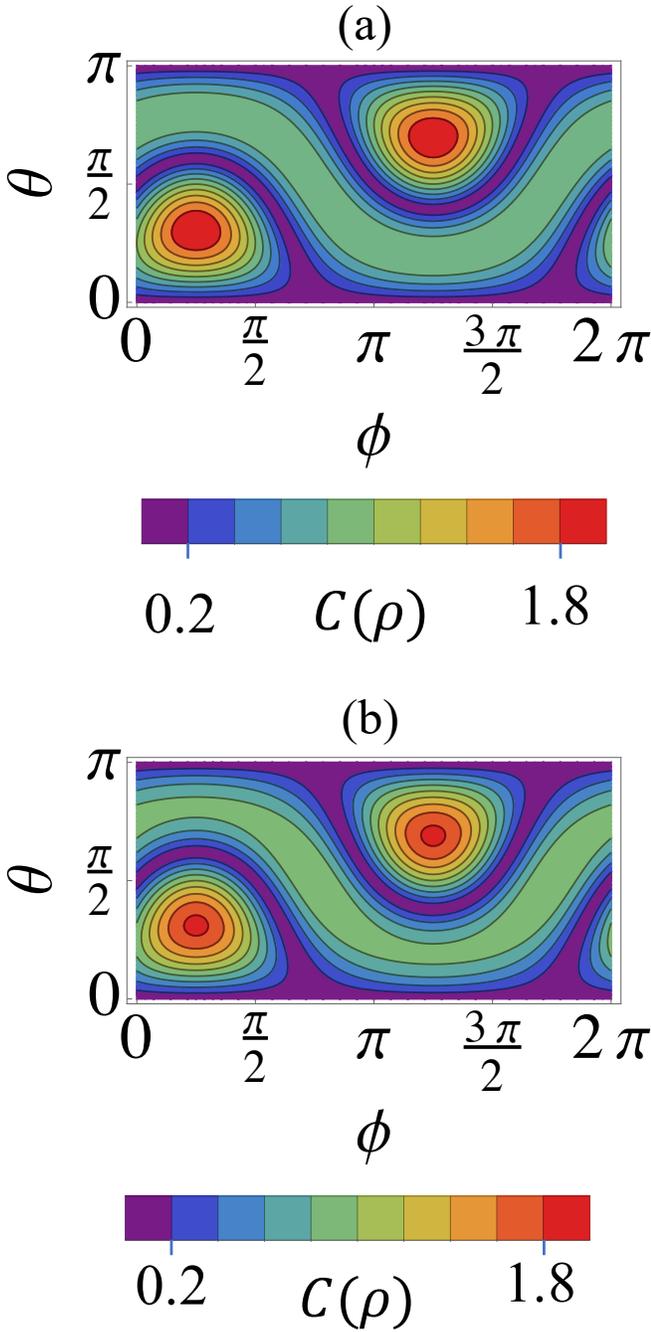
Figure 6: Contour plot of the Quantum coherence $C(\rho)$ as a function of θ and ϕ of the generalised W-state when one qubit is in a non-inertial frame is shown for (a) $r = 0.01$ and (b) $r = 4.0$.

the coherence of $\hat{\rho}_{BC}$ and the dashed lines denote the coherence in the state $\hat{\rho}_{AB}$. In Fig. 6 the contour plot shows the variation of quantum coherence as a function of the generalisation parameter θ and ϕ for the acceleration parameters $r = 0.01$ and $r = 4.0$.

Next we look at the case where two qubits, the ones

$$1.75 \quad C(\rho) \quad 1.95 \qquad 1.425 \quad C(\rho) \quad 1.65$$

$$1.175 \quad C(\rho) \quad 1.375 \qquad 1.6 \quad C(\rho) \quad 1.8$$
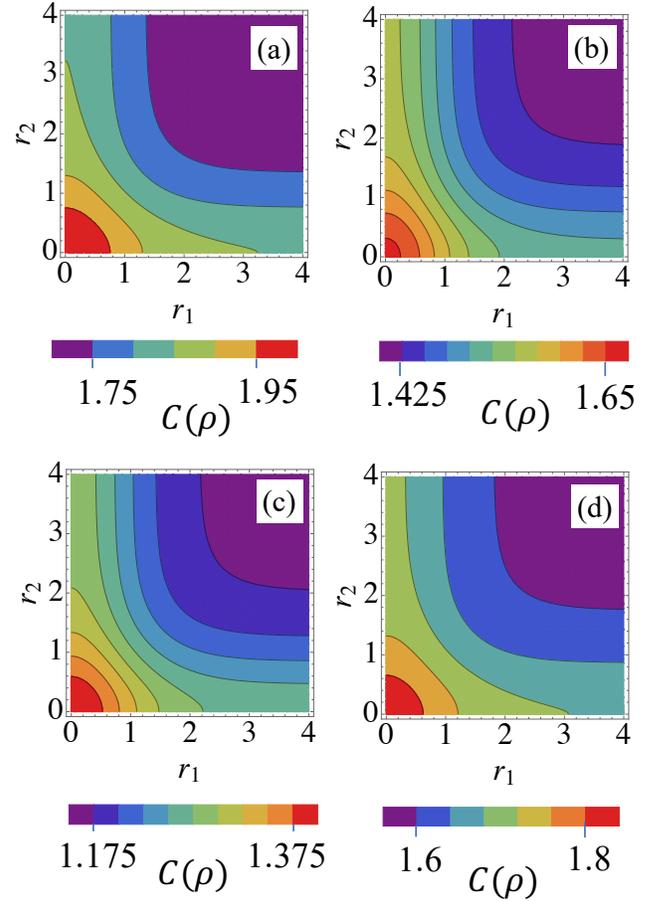
Figure 7: In the generalised W-state when both Bob's and Charlie's qubits are accelerated, the variation of quantum coherence as a function of the acceleration parameters r_1 and r_2 is given for (a) W-state, (b) $\theta = \pi/5$, $\phi = \pi/5$, (c) $\theta = \pi/6$, $\phi = \pi/6$ and (d) $\theta = \pi/3$, $\phi = \pi/6$.

corresponding to Bob and Charlie are being accelerated. Adopting a similar procedure of replacing the Minkowski states by Rindler modes and tracing out the Rindler second mode, we measure the total quantum coherence of the system. The quantum coherence of the tripartite system is,

$$
\begin{aligned}
C(\hat{\rho}) = {} & 2\sin\theta\cos\theta\sin\phi \\
& \times \frac{Li_{-1/2}(\tanh^2 r_1)}{\sinh^2 r_1 \cosh r_1} \frac{Li_{-1/2}(\tanh^2 r_2)}{\sinh^2 r_2 \cosh r_2} \\
& + 2\sin\theta\cos\theta\cos\phi \frac{Li_{-1/2}(\tanh^2 r_1)}{\sinh^2 r_1 \cosh r_1} \\
& + 2\sin^2\theta\sin\phi\cos\phi \frac{Li_{-1/2}(\tanh^2 r_2)}{\sinh^2 r_2 \cosh r_2}.
\end{aligned}
\tag{3.21}
$$

From Eq. (3.21) we notice that the quantum coherence is a sum of three terms. The first contains the non-inertial decoherence from both Bob's and Charlie's qubit. The non-inertial contributions from Bob and Charlie appear in the second and third terms respectively. At the bipartite level,

there are two possibilities namely: (i) when Alice's qubit is traced out; (ii) when either Bob's qubit or Charlie's qubit is traced out. The quantum coherence corresponding to these different situations are,

$$C(\hat{\rho}_{BC}) = 2 \sin\theta \cos\theta \sin\phi \frac{Li_{-1/2}(\tanh^2 r_1)}{\sinh^2 r_1 \cosh r_1}$$
$$\times \frac{Li_{-1/2}(\tanh^2 r_2)}{\sinh^2 r_2 \cosh r_2}, \qquad (3.22)$$

$$C(\hat{\rho}_{AC}) = 2 \sin\theta \cos\theta \sin\phi \frac{Li_{-1/2}(\tanh^2 r_1)}{\sinh^2 r_1 \cosh r_1}, \qquad (3.23)$$

$$C(\hat{\rho}_{AB}) = 2 \sin^2\theta \sin\phi \cos\phi \frac{Li_{-1/2}(\tanh^2 r_2)}{\sinh^2 r_2 \cosh r_2}. \qquad (3.24)$$

Here Eq. (3.22) refers to the situation where Alice's qubit is traced out and in the resulting bipartite system both the qubits are in non-inertial frames. When Bob's qubit is traced out the total quantum coherence is given through Eq. (3.23), and similarly when Charlie's qubit is traced out Eq. (3.24) gives the quantum coherence of the resulting bipartite state. For the W-state of the form $\frac{1}{\sqrt{3}}(|001\rangle + |010\rangle + |100\rangle)$ when both Bob's and Charlie's qubits are accelerated the total quantum coherence of the system is,

$$C(\hat{\rho}) = \frac{2}{3} \frac{Li_{-1/2}(\tanh^2 r_1)}{\sinh^2 r_1 \cosh r_1} \frac{Li_{-1/2}(\tanh^2 r_2)}{\sinh^2 r_2 \cosh r_2}$$
$$+ \frac{2}{3} \frac{Li_{-1/2}(\tanh^2 r_1)}{\sinh^2 r_1 \cosh r_1} + \frac{2}{3} \frac{Li_{-1/2}(\tanh^2 r_2)}{\sinh^2 r_2 \cosh r_2}. \qquad (3.25)$$

Eq. (3.25) reduces to the standard value of $C(\hat{\rho}) = 2$ for $r_1, r_2 \to 0$ and the single qubit acceleration limit when either r_1 or r_2 tends to zero. In the contour plot shown in Fig. 7 we analyse the variation of the quantum coherence as a function of r_1 and r_2 namely Charlie's and Bob's acceleration parameter for different values of the generalisation parameters θ and ϕ. We find that coherence is maximum when r_1 and r_2 are zero and decreases with increase in their value.

A very interesting limiting case of the generalised W-state occurs when $\theta = \pi/2$ and $\phi = \pi/4$. The generalised W-state corresponding to this value is $(|100\rangle + |010\rangle)/\sqrt{2}$. We can observe that this quantum state is of the biseparable form AB-C, where the AB pair is entangled and C is separable. In this state Charlie's qubit is accelerated, the total quantum coherence is $C = 1$. This is because the only coherence contribution in the system comes because of the correlation between Alice and Bob's qubit. On the contrary, when Bob is in a non-inertial frame of reference, the total quantum coherence in the system is,

$$C(\hat{\rho}) = \frac{Li_{-1/2}(\tanh^2 r)}{\sinh^2 r \cosh r}. \qquad (3.26)$$

When both Bob and Charlie are in non-inertial frames, the resulting coherence is same as when Bob is in a non-

inertial frame. This is because Charlie's qubit does not contribute to the coherence in the system.

For the W-state, the tripartite entanglement measured by the π-tangle saturates at a finite value [76]. This is in stark contrast with the results obtained for the bipartite entanglement in Ref. [31]. This is again due to the insufficiency in using π-tangle as a measure of entanglement. For a W-state, the variation of the quantum coherence due to uniform acceleration is similar to the change in the entanglement of the system. But the ℓ_1-norm measure of coherence is a complete measure unlike the π-tangle measure of entanglement used in Ref. [76]. The saturation nature of quantum coherence is due to the presence of non-classical correlations at relativistic velocities. This result holds for single qubit as well as two qubit accelerated systems.

IV. SEPARABLE STATES

The SLOCC class of classification applies to entangled states. But in general quantum states may not be entangled. An example of a separable state is $|000\rangle$ and for this state $\hat{\rho} = \hat{\rho}_d$ in the computational basis and so it is an incoherent state. Here we would like to mention that one of the crucial properties of quantum coherence is that it is a basis-dependent quantity. Hence studying a separable quantum state $|+++\rangle$ where $|+\rangle = (|0\rangle + |1\rangle)/\sqrt{2}$ in the σ^z-basis we find quantum coherence in the system. To find the relativistic effects, we accelerate either one or two of these qubits. For the accelerated qubits we replace the Minkowski states by their corresponding Rindler modes. We already know that there are two causally disconnected Rindler modes, so we trace out one of the modes and compute the quantum coherence of the rest of the system. Here when only Charlie's qubit is accelerated the quantum coherence computed using the ℓ_1-norm measure is,

$$C(\hat{\rho}) = 3 + \frac{4 Li_{-1/2}(\tanh^2 r)}{\cosh r \sinh^2 r}. \qquad (4.1)$$

In the $r \to 0$ limit, the inertial value of the ℓ_1-norm coherence of the system is recovered. When both Charlie's and Bob's qubit are accelerated the quantum coherence is,

$$C(\hat{\rho}) = 1 + \frac{2 Li_{-1/2}(\tanh^2 r_1)}{\cosh r_1 \sinh^2 r_1} + \frac{2 Li_{-1/2}(\tanh^2 r_2)}{\cosh r_2 \sinh^2 r_2}$$
$$+ \frac{2 Li_{-1/2}(\tanh^2 r_1)}{\cosh r_1 \sinh^2 r_1} \frac{Li_{-1/2}(\tanh^2 r_2)}{\cosh r_2 \sinh^2 r_2}. \qquad (4.2)$$

From this result, in the appropriate limiting conditions we can recover the single qubit result as well as the inertial value.

The coherence measured in the GHZ state, W-state and the separable $|+++\rangle$ state is the total amount of quantum coherence present in the states. But the type of coherence

in the GHZ and W-states is fundamentally different from the type of coherence present in the $|+++\rangle$ state. In the GHZ and W-states, the coherence arises due to the correlation between the qubits. Meanwhile the coherence in the $|+++\rangle$ state is because of the superposition between the levels within each qubit. These two fundamentally different forms of coherences were identified in Ref. [14]. The coherence arising due to the correlation between the qubits is the global coherence of the system and the coherence resulting from the superposition of the levels within a qubit are called local coherence. These two forms of coherences are complementary to each other in a sense that the increase in the global coherence causes a decrease in the local coherence and vice versa. With increase in the acceleration the quantum coherence decreases and it saturates at a finite value. To understand this for the $|+++\rangle$ state, we can consider the single qubit system $|+\rangle$ system which we can write as,

$$|+\rangle = \sum_{n=0}^{\infty} \frac{\tanh^n r}{\sqrt{2}\cosh r}\left(|n\rangle_I|n\rangle_{II} + \frac{\sqrt{n+1}}{\cosh r}|n+1\rangle_I|n\rangle_{II}\right). \tag{4.3}$$

Here we can observe that the initial superposition between two levels is spread out between the four modes. Of these two modes corresponding to Rindler region II are traced out and hence there is a loss of superposition and consequently a loss of coherence. This loss is the inaccessible coherence when the system undergoes uniform acceleration.

The GHZ and W-states represents one extreme where the global coherence is maximum with zero local coherence and the $|+++\rangle$ denotes the other extreme where the local coherence is maximum with no global coherence. But there are some pure quantum states in which both these types of coherence coexist. For such states we can quantify the global and local coherence using the formula,

$$C_G = \|\hat{\rho} - \pi(\hat{\rho})\|_{l_1}, \tag{4.4}$$
$$C_L = \|\pi(\hat{\rho}) - [\pi(\hat{\rho})]_d\|_{l_1}. \tag{4.5}$$

Here $\pi(\hat{\rho}) = \hat{\rho}_1 \otimes \cdots \otimes \hat{\rho}_N$ is the product state of the density matrix $\hat{\rho}$ where the reduced density matrix $\hat{\rho}_1 = \text{Tr}_{(2,\ldots,N)}\,\hat{\rho}$. The quantum state $[\pi(\hat{\rho})]_d$ is the decohered density matrix corresponding to $\pi(\hat{\rho})$ the product state. The total quantum coherence of the system C_T measures coherence contributions from correlations as well as local superpositions. In Ref. [14] a trade-off was observed between the global coherence and local coherence.

V. TRIPARTITE PURE STATES WITH LOCAL AND GLOBAL COHERENCE

In this section we study the non-inertial effects when both local and global coherences are present in the system. Towards this end we analyze the quantum coherence of tripartite $W\bar{W}$ and star states. The $W\bar{W}$ state is a symmetric tripartite state with both local and global coherence. On the contrary the star state is an asymmetric state with both local and global coherences.

V.1. $W\bar{W}$ state

The three qubit $W\bar{W}$ state [77] is a linear superposition of the tripartite W state and the $\bar{W}$ state as shown below,

$$|W\bar{W}\rangle = \frac{1}{\sqrt{2}}(|W\rangle + |\bar{W}\rangle),$$
$$|W\rangle = \frac{1}{\sqrt{3}}(|001\rangle + |010\rangle + |100\rangle),$$
$$|\bar{W}\rangle = \frac{1}{\sqrt{3}}(|011\rangle + |101\rangle + |110\rangle). \tag{5.1}$$

First we consider the situation, where a single qubit is in a noninertial frame that is to say only Charlie's qubit is being accelerated. After tracing out one of the Rindler region, the total quantum coherence of the resulting density matrix is,

$$C_T(\hat{\rho}) = 2 + \frac{3\,Li_{-1/2}(\tanh^2 r)}{\cosh r \sinh^2 r}. \tag{5.2}$$

In the $r \to 0$ limit the quantum coherence recovers the inertial limit.

The single qubit reduced density matrices of the $W\bar{W}$ state in Eq. (5.1) are,

$$\hat{\rho}_A = \hat{\rho}_B = \hat{\rho}_C = \begin{pmatrix} \frac{1}{2} & \frac{1}{3} \\ \frac{1}{3} & \frac{1}{2} \end{pmatrix}. \tag{5.3}$$

From the reduced density matrix we notice that the single qubit state has a finite amount of quantum coherence. Consequently the product state $\hat{\rho}_A \otimes \hat{\rho}_B \otimes \hat{\rho}_C$ will also have some coherence which is the local coherence of the system. Using Equations (4.4) and (4.5) we find the global and local coherence when one of the qubit is in non-inertial frame,

$$C_G(\hat{\rho}) = \frac{2}{9} + \frac{31\,Li_{-1/2}(\tanh^2 r)}{27\cosh r \sinh^2 r}, \tag{5.4}$$
$$C_L(\hat{\rho}) = \frac{16}{9} + \frac{50\,Li_{-1/2}(\tanh^2 r)}{27\cosh r \sinh^2 r}. \tag{5.5}$$

The behaviour of the total coherence, global coherence and local coherence are shown in Fig. 8(a). From the plots we find that all the different forms of coherences show identical behaviour and they decrease with increase in acceleration and attain a saturation value at higher values of acceleration. The results show that both global and local coherence have similar decoherence properties. Hence Unruh decoherence cannot distinguish between the two forms of coherence *viz* the one arising due to the correlations between the qubits and the quantumness due to the superposition between the levels within a qubit.
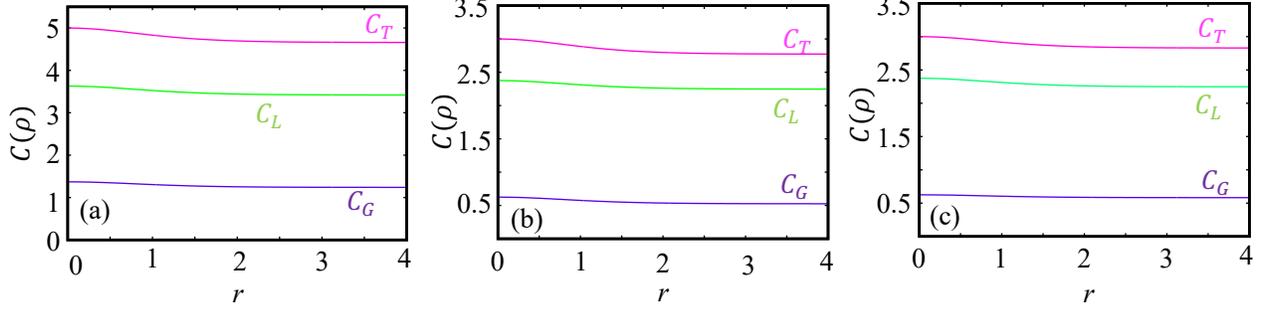
Figure 8: A plot of the total coherence (C_T), global coherence (C_G) and local coherence (C_L) for (a) the $W\bar{W}$ state, (b) Star state when the central qubit is accelerating and (c) Star state when the peripheral qubit is accelerating.

To study the relativistic effects when two qubits are in noninertial frames, we uniformly accelerate both Bob's and Charlie's qubits. The total quantum coherence of the $W\bar{W}$ state in this scenario is,

$$C_T(\hat{\rho}) = \frac{4}{6} + \frac{8\,Li_{-1/2}(\tanh^2 r_1)}{6\cosh r_1 \sinh^2 r_1} + \frac{8\,Li_{-1/2}(\tanh^2 r_2)}{6\cosh r_2 \sinh^2 r_2}$$
$$+ \frac{10 Li_{-1/2}(\tanh^2 r_1)\,Li_{-1/2}(\tanh^2 r_2)}{6\cosh r_1 \sinh^2 r_1\,\cosh r_2 \sinh^2 r_2}. \quad (5.6)$$

The total coherence is present as both global coherence arising from inter-qubit correlations and also as local coherence coming from intraqubit superpositions. The measured values of the global and local coherence of the system are,

$$C_G(\hat{\rho}) = \frac{2\,Li_{-1/2}(\tanh^2 r_1)}{9\cosh r_1 \sinh^2 r_1} + \frac{2\,Li_{-1/2}(\tanh^2 r_2)}{9\cosh r_2 \sinh^2 r_2}$$
$$+ \frac{25\,Li_{-1/2}(\tanh^2 r_1)\,Li_{-1/2}(\tanh^2 r_2)}{27\cosh r_1 \sinh^2 r_1\,\cosh r_2 \sinh^2 r_2}, \quad (5.7)$$

$$C_L(\hat{\rho}) = \frac{2}{3} + \frac{10\,Li_{-1/2}(\tanh^2 r_1)}{9\cosh r_1 \sinh^2 r_1} + \frac{10\,Li_{-1/2}(\tanh^2 r_2)}{9\cosh r_2 \sinh^2 r_2}$$
$$+ \frac{20\,Li_{-1/2}(\tanh^2 r_1)\,Li_{-1/2}(\tanh^2 r_2)}{27\cosh r_1 \sinh^2 r_1\,\cosh r_2 \sinh^2 r_2}. \quad (5.8)$$

We find that the total coherence, global coherence and local coherence reduce to their respective inertial values when $r_1, r_2 \to 0$. Also we find that the total coherence is a sum of the global and local coherence for the ℓ_1-norm of coherence.

V.2. Star state

A star state is an asymmetric quantum state [78, 79], so called because a central qubit is entangled with the peripheral qubits collectively, but upon tracing out the central qubit the peripheral ones have a separable form,

$$\hat{\rho}_{B,C} = \text{tr}_A(|S\rangle_{A,B,C}\langle S|_{A,B,C}) = \hat{\rho}_B \otimes \hat{\rho}_C. \quad (5.9)$$

In the tripartite star state we have a central qubit A which is entangled to other qubits B and C individually. The qubits B and C are not entangled with each other and are referred to as peripheral qubits. The form of the tripartite star state is,

$$|S\rangle = \frac{1}{2}(|000\rangle + |100\rangle + |101\rangle + |111\rangle). \quad (5.10)$$

When the central qubit A is accelerated, the total quantum coherence in the system is,

$$C_T(\hat{\rho}) = 1 + \frac{2\,Li_{-1/2}(\tanh^2 r)}{\cosh r \sinh^2 r}. \quad (5.11)$$

The star state has both global coherence and local coherence and they are

$$C_G(\hat{\rho}) = \frac{-1}{4} + \frac{7\,Li_{-1/2}(\tanh^2 r)}{8\cosh r \sinh^2 r}, \quad (5.12)$$

$$C_L(\hat{\rho}) = \frac{5}{4} + \frac{9\,Li_{-1/2}(\tanh^2 r)}{8\cosh r \sinh^2 r}. \quad (5.13)$$

When the peripheral qubit B is being accelerated, the total coherence of the system calculated using the ℓ_1-norm of coherence is,

$$C_T(\hat{\rho}) = \frac{3}{2} + \frac{3\,Li_{-1/2}(\tanh^2 r)}{2\cosh r \sinh^2 r}. \quad (5.14)$$

The corresponding global of the system is,

$$C_G(\hat{\rho}) = \frac{1}{4} + \frac{3\,Li_{-1/2}(\tanh^2 r)}{8\cosh r \sinh^2 r}. \quad (5.15)$$

The local coherence of the system on accelerating the peripheral qubit is same as the local coherence when the central qubit is being under acceleration, the expression for which is given in Eq. (5.13). In both the cases namely when the central qubit and the peripheral qubit in the $r \to 0$ limit the results corresponding to the inertial frame are recovered. For the star states, the variation of quantum coherence is qualitatively similar when both the

central and peripheral qubits are accelerated. The global local and total coherence have a maximum value in the inertial frame and decreases with acceleration and attain a saturation value for large values of the acceleration as shown in Fig. 8. From the analysis of the two different situations where either the central qubit or the peripheral qubit is being accelerated, we find that both global and local coherence have similar decoherence properties. This shows that Unruh decoherence affects all kinds of quantumness equally.

Next we look at the situation where two qubits are in non-inertial frames of reference. Due to the asymmetry of the star states, there are two possibilities for this situation *viz*: (i) when a peripheral qubit and a central qubit are accelerated ; (ii) when both the peripheral qubits are accelerated. The first situation can be analysed when both Bob's and Charlie's qubits are simultaneously accelerated. The total coherence of the system in this case is,

$$
C_T(\hat{\rho}) = \frac{1}{2} + \frac{Li_{-1/2}(\tanh^2 r_1)}{\cosh r_1 \sinh^2 r_1} + \frac{1}{2}\frac{Li_{-1/2}(\tanh^2 r_2)}{\cosh r_2 \sinh^2 r_2} + \frac{Li_{-1/2}(\tanh^2 r_1)}{\cosh r_1 \sinh^2 r_1}\frac{Li_{-1/2}(\tanh^2 r_2)}{\cosh r_2 \sinh^2 r_2}. \quad (5.16)
$$

Under the same conditions the global and local coherence of the star state are,

$$
C_G(\hat{\rho}) = \frac{1}{2} + \frac{1}{4}\frac{Li_{-1/2}(\tanh^2 r_1)}{\cosh r_1 \sinh^2 r_1} - \frac{1}{4}\frac{Li_{-1/2}(\tanh^2 r_1)}{\cosh r_2 \sinh^2 r_2} + \frac{5}{8}\frac{Li_{-1/2}(\tanh^2 r_1)\,Li_{-1/2}(\tanh^2 r_2)}{\cosh r_1 \sinh^2 r_1\,\cosh r_2 \sinh^2 r_2}, \quad (5.17)
$$

$$
C_L(\hat{\rho}) = \frac{1}{2} + \frac{3}{4}\frac{Li_{-1/2}(\tanh^2 r_1)}{\cosh r_1 \sinh^2 r_1} + \frac{3}{4}\frac{Li_{-1/2}(\tanh^2 r_2)}{\cosh r_2 \sinh^2 r_2} + \frac{3}{8}\frac{Li_{-1/2}(\tanh^2 r_1)\,Li_{-1/2}(\tanh^2 r_2)}{\cosh r_1 \sinh^2 r_1\,\cosh r_2 \sinh^2 r_2}. \quad (5.18)
$$

In the second case when Alice and Bob's qubits are being accelerated, the total coherence of the system is,

$$
C_T(\hat{\rho}) = \frac{1}{2} + \frac{Li_{-1/2}(\tanh^2 r_1)}{\cosh r_1 \sinh^2 r_1} + \frac{Li_{-1/2}(\tanh^2 r_2)}{\cosh r_2 \sinh^2 r_2} + \frac{1}{2}\frac{Li_{-1/2}(\tanh^2 r_1)}{\cosh r_1 \sinh^2 r_1}\frac{Li_{-1/2}(\tanh^2 r_2)}{\cosh r_2 \sinh^2 r_2}. \quad (5.19)
$$

The corresponding global and local coherences are,

$$
C_G(\hat{\rho}) = \frac{Li_{-1/2}(\tanh^2 r_1)}{4\cosh r_1 \sinh^2 r_1} + \frac{Li_{-1/2}(\tanh^2 r_2)}{4\cosh r_2 \sinh^2 r_2} + \frac{Li_{-1/2}(\tanh^2 r_1)\,Li_{-1/2}(\tanh^2 r_2)}{8\cosh r_1 \sinh^2 r_1\,\cosh r_2 \sinh^2 r_2}, \quad (5.20)
$$

$$
C_L(\hat{\rho}) = \frac{1}{2} + \frac{3\,Li_{-1/2}(\tanh^2 r_1)}{4\cosh r_1 \sinh^2 r_1} + \frac{3\,Li_{-1/2}(\tanh^2 r_2)}{4\cosh r_2 \sinh^2 r_2} + \frac{3\,Li_{-1/2}(\tanh^2 r_1)\,Li_{-1/2}(\tanh^2 r_2)}{8\cosh r_1 \sinh^2 r_1\,\cosh r_2 \sinh^2 r_2}. \quad (5.21)
$$
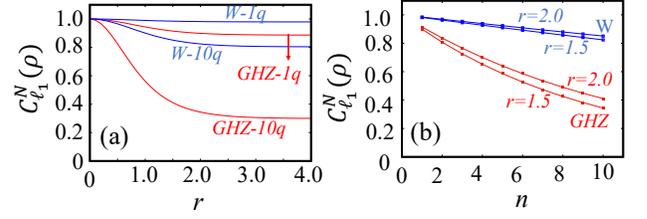
Figure 9: A plot of the variation of the normalized decoherence (a) with the acceleration parameter r and (b) with the number of accelerated qubits n for a fixed values of $r = 1.5$ and $r = 2.0$. The total number of qubits in the system is $N = 11$.

All the different quantum coherences attain their inertial values in the limit $r \to 0$. From the expressions of the total, global and local coherence we find that the $C_T = C_G + C_L$ for all the different cases of star states.

In the tripartite systems like $W\bar{W}$-states and star states, the total coherence in the system is distributed as global and local coherence. Here by the word global coherence we mean coherence arising due to all the types of non-classical correlations (both local and entanglement type) between the qubits. Hence the global coherence does not fall to zero in the infinite acceleration limit and rather saturates to a finite value due to the presence of local correlations. The effect of non-inertial motion on local coherence has not been investigated before. From our results we can see that the intra-qubit superpositions do not completely vanish in the infinite acceleration limit which is a very interesting result. In the tripartite systems when either one or two of the parties are in non-inertial frames of reference, the accelerated qubits get split into two modes corresponding to the two Rindler regions. The degradation of quantum coherence is because part of the coherence becomes inaccessible to experimental measurement. Both the global and local coherence decay at the same rate. Hence we find that the acceleration affects the interqubit and intraqubit properties in the same manner.

VI. APPLICATIONS

VI.1. Relativistic effects on multipartite state distributed over a network

Let us consider a network of satellites sharing a multipartite quantum state. An important study, could be about the effect of acceleration on the quantum coherence of the multipartite system. To understand this, we measure the quantum coherence of the N-partite GHZ and W-state. In the N partite state, we have n number of uniformly accelerated qubits. First let us consider a N-partite GHZ state,

$$
|\text{GHZ}\rangle = \frac{1}{\sqrt{2}}(|0\rangle^{\otimes N} + |1\rangle^{\otimes N}). \quad (6.1)
$$

The total quantum coherence is $C_{\ell_1}(\hat{\rho}) = 1$ for this state. Out of the N-qubits if n qubits undergo acceleration, the quantum coherence of the state is,

$$C(\hat{\rho}) = \prod_{k=1}^{n} \frac{Li_{-1/2}(\tanh^2 r_k)}{\sinh^2 r_k \cosh r_k}. \tag{6.2}$$

Let $C_k(\hat{\rho})$ be the quantum coherence of the N-partite system when only the kth qubit is being accelerated. Using this the coherence of the N-partite system with n accelerating qubits can be written as,

$$C(\hat{\rho}) = \prod_{k=1}^{n} C_k(\hat{\rho}). \tag{6.3}$$

When all the satellites have the same acceleration, the quantum coherence simplifies to $C(\hat{\rho}) = [C_k(\hat{\rho})]^n$. From this result we can see that the quantum coherence of the N-partite GHZ state falls exponentially with the increase in the number of accelerating satellites. This exponential fall is a manifestation of genuinely multipartite form of quantum coherence where the loss of even a single qubit makes the state completely incoherent. Hence a small acceleration of each of the m qubits leads to a huge loss of coherence in the whole system. To put this into a numerical perspective let us consider a 11 qubit GHZ state without any of the qubits under acceleration. The quantum coherence of such a system is $C_{\ell_1}(\hat{\rho}) = 1$ and let us consider $r = 2.0$ for each of the qubit. The coherence when only one qubit is accelerating is $C_{\ell_1}(\hat{\rho}) = 0.8988$. Now when 10 qubits start accelerating, we can see that the total coherence reduced to $C_{\ell_1}(\hat{\rho}) = (0.8988)^{10} = 0.3439$. For very large values of n, the quantum coherence $C_{\ell_1} \to 0$. Since the reduction of quantum coherence depends on its distribution in multipartite system, the results obtained here might hold for entanglement as well. This is because coherence and entanglement are distributed in a similar manner. So we can expect entanglement to fall exponentially similar to quantum coherence. Hence when quantum information is shared between a network of satellites, the quantum coherence is a function of the number of accelerating satellites and the amount of acceleration.

Next we consider the N-partite W-state,

$$|W\rangle = \frac{1}{\sqrt{N}}(|00\cdots01\rangle + |00\cdots10\rangle + \cdots + |10\cdots00\rangle). \tag{6.4}$$

In the non-relativistic scenario the total quantum coherence of this state in the non-inertial frame of reference is $C_{\ell_1}(\hat{\rho}) = N - 1$. Here if n qubits start accelerating, the quantum coherence of the N-partite state changes to,

$$
\begin{aligned}
C_{\ell_1}(\hat{\rho}) = & \frac{2}{N} \sum_{\substack{1 \le i,j \le n \\ i<j}} \frac{Li_{-1/2}(\tanh^2 r_i)}{\sinh^2 r_i \cosh r_i} \frac{Li_{-1/2}(\tanh^2 r_j)}{\sinh^2 r_j \cosh r_j} \\
& + \frac{2}{N}(N-n) \sum_{i=1}^{N} \frac{Li_{-1/2}(\tanh^2 r_i)}{\sinh^2 r_i \cosh r_i} \\
& + \frac{(N-n)(N-(n+1))}{N}.
\end{aligned} \tag{6.5}
$$

In the large N limit, when $n \approx N$ the first term which is a product of two polylog functions dominates over the second and the third term. Hence we would see the quantum coherence falling as polynomial function of second order. When $n \ll N$ in the large N limit, the third term dominates over the first and second term. Consequently the decrease of quantum coherence due to the relativistic effects will be minimal under such situations. If acceleration is the same for all the satellites then we have,

$$
\begin{aligned}
C_{\ell_1}(\hat{\rho}) = & \frac{2}{N} \frac{n(n-1)}{2} \left[\frac{Li_{-1/2}(\tanh^2 r_i)}{\sinh^2 r_i \cosh r_i} \right]^2 \\
& + \frac{2}{N}(N-n)n \left[\frac{Li_{-1/2}(\tanh^2 r_i)}{\sinh^2 r_i \cosh r_i} \right] \\
& + \frac{(N-n)(N-(n+1))}{N}.
\end{aligned} \tag{6.6}
$$

Since the quantum coherence of the N-partite W-state is $(N-1)$, it is not possible to compare it with the coherence loss of the GHZ state. To make a comparison between the coherence loss of the GHZ and W-states we define,

$$C_{\ell_1}^{N}(\hat{\rho}) = \frac{C_{\ell_1}^{R}(\hat{\rho})}{C_{\ell_1}^{NR}(\hat{\rho})}, \tag{6.7}$$

where $C_{\ell_1}^{N}$ is the normalized amount of quantum coherence and $C_{\ell_1}^{R}$ is the amount of relativistic coherence and $C_{\ell_1}^{NR}$ is the quantum coherence of the non-relativistic state. For the GHZ state $C_{\ell_1}^{NR} = 1$ and so $C_{\ell_1}^{N}(\hat{\rho}) = C_{\ell_1}^{R}(\hat{\rho})$. In the case of the W-state, for $r = 2.0$, $C_{\ell_1}^{R}(\hat{\rho}) = 8.2430$ and $C_{\ell_1}^{NR} = N - 1$. The normalized amount of quantum coherence in the system when 10 out of 11 qubits are being accelerated is $C_{\ell_1}^{N} = 0.8243$. Hence, for the same number of quantum states and acceleration, we find that the quantum coherence of W-state is more robust to Unruh decoherence when compared with GHZ state. This implies that in a multipartite system sharing quantum coherence in a bipartite manner protects it from decoherence due to relativistic effects.

Figs. 9(a) and 9(b) depicts the relativistic quantum coherence of the system. In Fig. 9(a) we plot the change in quantum coherence with r for both GHZ and W-states. Here we consider two situations where one qubit is being accelerated or 10 qubits are being accelerated. In the first

case, where one qubit is under acceleration the loss of coherence is minimal. Compared to the first case, we find that the coherence loss is much higher when 10 qubits are accelerated. Also we find that among these states, the W-state with increasing accelerating qubits is more robust to decoherence. In Fig. 9 (b) we plot the coherence as a function of the number of accelerating qubits. We find that the loss of coherence is higher with increase in the number of accelerating qubits. Also for a given number of accelerating qubits, the GHZ states experience a higher loss of coherence.

VI.2. Coherence degradation at infinite acceleration

The entanglement degradation in the highly relativistic situation has been explained in Ref. [31] in the context of a bipartite systems. In Ref. [31], the authors consider the two qubit case where Alice is an inertial observer and Bob being non-inertial with uniform acceleration. In the infinite acceleration limit, non-inertial Bob is close to the Rindler horizon Ref. [31], which can be considered as the event horizon from the perspective of a black hole. It is well known that a spherical non-rotating static black hole can be described using a Schwarzschild space-time. This can be approximated by Rindler co-ordinate in Minkowski space-time in the infinite acceleration limit [80]. Hence in the existing scenario, we consider Alice and Bob to be close to the event horizon, such that inertial Alice falls into a static black hole and accelerating Bob close to event horizon escapes from falling into it.

Similarly our work investigates the quantum coherence degradation in tripartite systems due to relativistic effects. Here we consider three qubits, one each in the possession of Alice, Bob and Charlie. Degradation of quantum coherence has been observed when either a single qubit or two qubits are being accelerated. From our results in Sec. III, for both GHZ and W-states we notice a decrease in quantum coherence, but the coherence freezes at a finite amount in the infinite acceleration limit. The entire coherence in the GHZ and W-state is due to the correlations between the qubits. In a similar context to understand the relativistic effects on local coherence we study the $|+++\rangle$ separable state. The qualitative behavior of the local coherence in the $|+++\rangle$ state is similar to that of the global coherence of the GHZ and W-states. Hence we conclude that when an inertial observer falls into a black hole, the quantum correlations and quantum superposition shared with the non-inertial observer does not vanish completely.

VII. RESULTS & DISCUSSION

The relativistic effects on the quantum coherence of a multipartite system is investigated using the ℓ_1-norm measure of coherence. Initially all the qubits are in an inertial frame and can be described using Minkowski space-time coordinates. When some of the qubits are under acceleration, the Minkowski space corresponding to them is divided into two causally disconnected regions. From the Minkowski modes, the Rindler modes can be obtained via the Unruh modes. When we consider a Gaussian Minkowski smearing function it can be approximated by a single Unruh mode. Under the monochromatic approximation we can describe the states using Rindler co-ordinates in the Minkowski space time. Hence the quantum coherence initially present in the Minkowski co-ordinates is distributed between the two Rindler co-ordinates of which only one is experimentally accessible. The coherence which can be measured in the accessible Rindler region is called the accessible coherence. The coherence corresponding to the other Rindler region is called the inaccessible coherence since it cannot be experimentally measured.

First we investigate the tripartite quantum systems. Based on the SLOCC classification, the tripartite states are classified into the GHZ class and the W classes. For both the GHZ and W-states we find that the quantum coherence decreases with increase in acceleration and attains a saturation value for very high accelerations. Here we note that coherence can exist due to correlations between qubits which is known as global coherence. Also coherence may arise due to superposition between the levels within a qubit, referred to as local coherence. The global coherence is the only coherence present in the GHZ and the W-states.

Next we consider a separable state of the form $|+++\rangle$, to understand the relativistic effects on local coherence. The local coherence also decreases with increase in acceleration and saturates at higher acceleration. The local coherence and the global coherence are complementary to each other and the total coherence is a combination of these two types of coherences. Some tripartite quantum states have both local and global coherence. As an example we consider two such quantum states namely $W\bar{W}$ and star states. In the $W\bar{W}$ state, the global coherence is distributed equally between the three qubits. There is an asymmetric distribution of quantum coherence in the star states. For both these states, all the different forms of coherence namely the global, local and total coherence decreases with an increase in acceleration.

The entanglement of the bipartite system decreases due to relativistic effects and reaches zero in the infinite acceleration limit [31]. But the tripartite entanglement measured in Ref. [76] using the π-tangle does not go to zero for higher values of acceleration. Due to relativistic effects the quantum discord of a system also does not go to zero in the infinite acceleration limit [55]. For the tripartite entanglement, the non-vanishing nature is because the π-tangle is not a complete measure of entanglement. But for the quantum discord this is a fundamental feature of the underlying quantum correlations. From our work we find that there is a qualitative relationship between the total quantum correlations and the quantum coherence
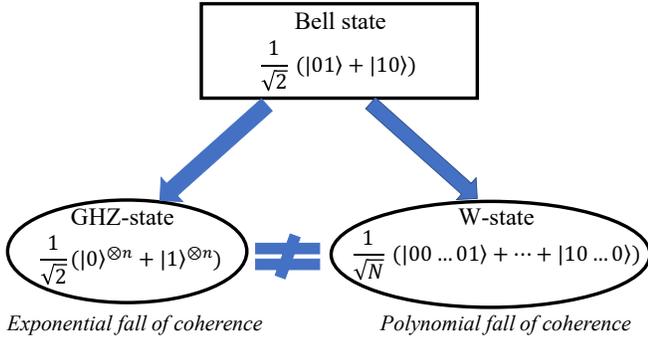
Figure 10: A schematic illustration of the bifurcation of the Bell state which displays linear loss of coherence into two extreme classes of states *viz.* GHZ class with exponential loss of coherence and W class with polynomial loss of coherence.

of a relativistic quantum system.

In quantum information theory, it is not possible to distinguish between Bell states and the GHZ states through an estimation of entropy. But we can calculate the quantum coherence of these two states when they are in an inertial frame of reference. Here we again find that $C(|\psi_{Bell}\rangle) = C(|\psi_{GHZ}\rangle)$ and so we will not be able to distinguish between these two states. This is because the GHZ state $\frac{1}{\sqrt{2}}(|000\rangle + |111\rangle)$ can be rewritten as an equivalent Bell state $\frac{1}{\sqrt{2}}(|\mathbf{0}\mathbf{0}\rangle + |\mathbf{1}\mathbf{1}\rangle)$ where $|\mathbf{0}\rangle = |00\rangle$ and $|\mathbf{1}\rangle = |11\rangle$ are redundantly encoded logical qubits encoding the same quantum information. Next we consider the situation where part of the system is moving with constant acceleration. When the single qubit in GHZ and Bell states move with constant acceleration it is not possible to distinguish between them. On the contrary when the logical qubit of the GHZ state is in an accelerated motion, then we have $C(|\psi_{Bell}\rangle) \neq C(|\psi_{GHZ}\rangle)$ and the reason for this is that the size of the logical qubit under uniform acceleration is bigger than that of the regular qubit of the Bell state. This result is very interesting from a quantum information theory perspective where in general we cannot distinguish between Bell and GHZ states or between multipartite GHZ states with different number of qubits. But a measurement of quantum coherence combined with relativistic motion can differentiate them. Thus coherence measurement of accelerated systems can be used in quantum state discrimination.

Next we consider a N-partite GHZ state and W-state and estimate the quantum coherence when $n < N$ qubits are accelerated. The GHZ and W-state represent the two extremes of coherence sharing. In the GHZ state, the coherence is present in a maximally entangled multipartite manner such that the loss of a single qubit destroys the entire coherence in the system. We find that in a GHZ state when the number of accelerating qubits n increases, the coherence falls exponentially. The coherence in a W-state is shared in a local bipartite fashion. Here in the case of a W-states we observe that the coherence falls polynomially with increase in the number of accelerating

qubits. In Fig. 10, through a flow chart style we illustrate the quantum coherence decrease as we move from $n = 2$ to $n > 2$ quantum system.

The Bell states describe the maximally entangled states in a two qubit system. When one of the qubits becomes non-inertial, then the coherence of the Bell state is given by $C_{\ell_1} = Li_{-1/2}(\tanh^2 r)/(\sinh^2 r \cosh r)$. There is only one way to entangle or correlate in a bipartite state. When we move to multipartite systems, there is more than one way to correlate the states. The GHZ and W-states denote the two extreme forms of correlation sharing where it is shared in a multipartite fashion in the former case and in a bipartite manner in the later one. When more than one qubit is accelerated, the coherence falls exponentially in the GHZ state and polynomially in the W-state. As we move from the bipartite to the multipartite case, the linear fall of coherence observed in Bell type states changes to exponential fall for the GHZ states and polynomial decrease for the W-state. Hence the Bell type maximally entangled state clearly bifurcates into two extreme classes of entangled states with exponential fall (GHZ class) and polynomial fall (W-state) of coherence. This also proves that the W-state is more robust to Unruh decoherence compared to the GHZ state. This is because the coherence is shared in a genuinely multipartite manner in a GHZ state, but in a W-state it is shared only in a bipartite way. For large N W-state, the loss of a few qubits results in a W-like state. This result might be useful for satellite based quantum communication, where some of the satellites are moving with very high velocities. In Ref. [81] the quantum coherence of multipartite W-states for Dirac field has been calculated in terms of the Kruskal modes in certain limiting cases. But in our work, we consider multipartite W-states of bosonic modes and compute quantum coherence in a very general setting where arbitrary number of qubits are being accelerated. In our method the Minkowski modes are converted into Rindler modes in the noninertial frame.

A spherical non-rotating blackhole is described by a Schwarzchild space-time. In the infinite acceleration limit, the Schwarzchild space-time can be approximately described by Rindler co-ordinates in Minkowski space time. Hence our investigation in the infinite acceleration limit can be used to analyze quantum coherence in the context of black holes. Our study shows that when Alice falls into a black hole, she might still share quantum coherence with Bob and Charlie who are escaping from the black-hole. Hence we conclude that quantum correlations and quantum superposition present in a system do not completely vanish in the relativistic limit.

In our work we have used the single mode approximation where we use single frequency global modes. This can be experimentally realized using localized sources and detectors. Some proposals towards this end might include the use of localized projective measurements [82], homodyne detection [51] and accelerated cavities [83, 84]. Here we note that for a pure state, the l_1 norm measure of coherence is equal to the robustness of coherence [73],

which can be directly estimated using the interference of fringes. A possible method is the use of Berry phase atomic interferometry experiment [85, 86], in which one of arm of the interferometer is under non-inertial motion. The phase difference between the inertial and non-inertial arms can give us the change in coherence due to the non-inertial motion. Hence an experimental verification of relativistic effects on quantum coherence might be an interesting future work. On the theoretical side an investigation on the quantum coherence effects in curved space time is also an interesting topic to explore.

[1] P. W. Shor, Quantum computing, Documenta Mathematica **1**, 467 (1998).

[2] D. Deutsch and R. Jozsa, Rapid solution of problems by quantum computation, Proceedings of the Royal Society of London. Series A: Mathematical and Physical Sciences **439**, 553 (1992).

[3] L. K. Grover, A fast quantum mechanical algorithm for database search, in *Proceedings of the twenty-eighth annual ACM symposium on Theory of computing* (1996) pp. 212–219, quant-ph/9605043.

[4] P. W. Shor, Polynomial-time algorithms for prime factorization and discrete logarithms on a quantum computer, SIAM Review **41**, 303 (1999), quant-ph/9508027.

[5] V. Giovannetti, S. Lloyd, and L. Maccone, Quantum metrology, Physical Review Letters **96**, 010401 (2006), quant-ph/0509179.

[6] C. H. Bennett, G. Brassard, C. Crépeau, R. Jozsa, A. Peres, and W. K. Wootters, Teleporting an unknown quantum state via dual classical and einstein-podolsky-rosen channels, Physical Review Letters **70**, 1895 (1993).

[7] D. Bouwmeester, J.-W. Pan, K. Mattle, M. Eibl, H. Weinfurter, and A. Zeilinger, Experimental quantum teleportation, Nature **390**, 575 (1997), 1901.11004.

[8] C. H. Bennett and G. Brassard, Quantum cryptography: Public key distribution and con tos5, in *Proceedings of the International Conference on Computers, Systems and Signal Processing* (1984) pp. 175–179.

[9] C. H. Bennett, F. Bessette, G. Brassard, L. Salvail, and J. Smolin, Experimental quantum cryptography, Journal of Cryptology **5**, 3 (1992).

[10] J.-D. Bancal, C. Branciard, N. Gisin, and S. Pironio, Quantifying multipartite nonlocality, Physical Review Letters **103**, 090503 (2009), 0903.2715.

[11] P. Skrzypczyk, M. Navascués, and D. Cavalcanti, Quantifying einstein-podolsky-rosen steering, Physical Review Letters **112**, 180404 (2014).

[12] H. Ollivier and W. H. Zurek, Quantum discord: a measure of the quantumness of correlations, Physical Review Letters **88**, 017901 (2001).

[13] T. Baumgratz, M. Cramer, and M. B. Plenio, Quantifying coherence, Physical Review Letters **113**, 140401 (2014).

[14] C. Radhakrishnan, M. Parthasarathy, S. Jambulingam, and T. Byrnes, Distribution of quantum coherence in multipartite systems, Physical Review Letters **116**, 150504 (2016).

[15] A. Winter and D. Yang, Operational resource theory of coherence, Physical Review Letters **116**, 120404 (2016), 1506.07975.

[16] F. G. Brandão and G. Gour, Reversible framework for quantum resource theories, Physical Review Letters **115**, 070503 (2015).

[17] E. Chitambar and G. Gour, Critical examination of incoherent operations and a physically consistent resource theory of quantum coherence, Physical Review Letters **117**, 030401 (2016).

[18] E. Chitambar and M.-H. Hsieh, Relating the resource theories of entanglement and quantum coherence, Physical Review Letters **117**, 020402 (2016).

[19] T. Chanda and S. Bhattacharya, Delineating incoherent non-markovian dynamics using quantum coherence, Annals of Physics **366**, 1 (2016), 1505.05810.

[20] C. Radhakrishnan, Z. Lü, J. Jing, and T. Byrnes, Dynamics of quantum coherence in a spin-star system: Bipartite initial state and coherence distribution, Physical Review A **100**, 042333 (2019).

[21] M. Hillery, Coherence as a resource in decision problems: The deutsch-jozsa algorithm and a variation, Physical Review A **93**, 012111 (2016), 1512.01874.

[22] C. Zhang, T. R. Bromley, Y.-F. Huang, H. Cao, W.-M. Lv, B.-H. Liu, C.-F. Li, G.-C. Guo, M. Cianciaruso, and G. Adesso, Demonstrating quantum coherence and metrology that is resilient to transversal noise, Physical Review Letters **123**, 180504 (2019), 1907.10540.

[23] J. Ma, Y. Zhou, X. Yuan, and X. Ma, Operational interpretation of coherence in quantum key distribution, Physical Review A **99**, 062325 (2019), 1810.03267.

[24] A. Peres and D. R. Terno, Quantum information and relativity theory, Reviews of Modern Physics **76**, 93 (2004).

[25] J. Dunningham, V. Palge, and V. Vedral, Entanglement and nonlocality of a single relativistic particle, Physical Review A **80**, 044302 (2009).

[26] R. B. Mann and T. C. Ralph, Relativistic quantum information, Classical and Quantum Gravity **29**, 220301 (2012).

[27] P. M. Alsing and G. J. Milburn, Lorentz invariance of entanglement, arXiv preprint quant-ph/0203051 10.26421/qic2.6-4 (2002), quant-ph/0203051.

[28] P. M. Alsing and I. Fuentes, Observer-dependent entanglement, Classical and Quantum Gravity **29**, 224001 (2012), 1210.2223.

[29] H. Li and J. Du, Relativistic invariant quantum entanglement between the spins of moving bodies, Physical Review A **68**, 022108 (2003), quant-ph/0211159.

[30] Y. Shi, Entanglement in relativistic quantum field theory, Physical Review D **70**, 105001 (2004), hep-th/0408062.

[31] I. Fuentes-Schuller and R. B. Mann, Alice falls into a black hole: entanglement in noninertial frames, Physical Review Letters **95**, 120404 (2005), quant-ph/0410172.

[32] D. E. Bruschi, J. Louko, E. Martín-Martínez, A. Dragan, and I. Fuentes, Unruh effect in quantum information beyond the single-mode approximation, Phys. Rev. A **82**, 042332 (2010).

[33] A. Dragan, J. Doukas, E. Martín-Martínez, and D. E. Bruschi, Localized projective measurement of a quantum field in non-inertial frames, Classical and Quantum Gravity **30**, 10.1088/0264-9381/30/23/235006 (2013).

[34] G.-H. S. . S.-H. D. Qian Dong, Ariadna J. Torres-Arenas, Tetrapartite entanglement features of w-class state in uniform acceleration, Front. Phys. **15**, 11602 (2020).

[35] W. G. Unruh, Notes on black-hole evaporation, Phys. Rev. D **14**, 870 (1976).

[36] T. G. Downes, T. C. Ralph, and N. Walk, Quantum communication with an accelerated partner, Physical Review A **87**, 10.1103/physreva.87.012327 (2013).

[37] D. Kabat, Black hole entropy and entropy of entanglement, Nuclear Physics B **453**, 281 (1995), hep-th/9503016.

[38] L. J. Henderson, R. A. Hennigar, R. B. Mann, A. R. Smith, and J. Zhang, Harvesting entanglement from the black hole vacuum, Classical and Quantum Gravity **35**, 21LT02 (2018), 1712.10018.

[39] E. Martín-Martínez, L. J. Garay, and J. León, Unveiling quantum entanglement degradation near a schwarzschild black hole, Physical Review D **82**, 064006 (2010).

[40] E. Martín-Martínez, L. J. Garay, and J. León, Quantum entanglement produced in the formation of a black hole, Physical Review D **82**, 064028 (2010).

[41] H. Terashima, Entanglement entropy of the black hole horizon, Physical Review D **61**, 104016 (2000), gr-qc/9911091.

[42] E. Verlinde and H. Verlinde, Black hole entanglement and quantum error correction, Journal of High Energy Physics **2013**, 107 (2013), 1211.6913.

[43] M. Ahmadi, D. E. Bruschi, C. Sabín, G. Adesso, and I. Fuentes, Relativistic quantum metrology: Exploiting relativity to improve quantum measurement technologies, Scientific Reports **4**, 1 (2014).

[44] M. Ahmadi, D. E. Bruschi, and I. Fuentes, Quantum metrology for relativistic quantum fields, Physical Review D **89**, 065028 (2014), 1312.5707.

[45] Z. Tian, J. Wang, H. Fan, and J. Jing, Relativistic quantum metrology in open system dynamics, Scientific Reports **5**, 1 (2015), 1501.06676.

[46] H. Du and R. B. Mann, Fisher information as a probe of spacetime structure: relativistic quantum metrology in (a) ds, Journal of High Energy Physics **2021**, 1 (2021), 2012.08557.

[47] N. Friis, A. R. Lee, K. Truong, C. Sabín, E. Solano, G. Johansson, and I. Fuentes, Relativistic quantum teleportation with superconducting circuits, Physical Review Letters **110**, 113602 (2013).

[48] S.-Y. Lin, C.-H. Chou, and B. Hu, Quantum teleportation between moving detectors, Physical Review D **91**, 084063 (2015).

[49] P. T. Grochowski, G. Rajchel, F. Kiałka, and A. Dragan, Effect of relativistic acceleration on continuous variable quantum teleportation and dense coding, Physical Review D **95**, 105005 (2017).

[50] J.-i. Koga, G. Kimura, and K. Maeda, Quantum teleportation in vacuum using only unruh-dewitt detectors, Physical Review A **97**, 062338 (2018), 1804.01183.

[51] T. Downes, T. Ralph, and N. Walk, Quantum communication with an accelerated partner, Physical Review A **87**, 012327 (2013), 1203.2716.

[52] A. G. Landulfo, Nonperturbative approach to relativistic quantum communication channels, Physical Review D **93**, 104019 (2016).

[53] K. Kravtsov, I. Radchenko, S. Kulik, and S. Molotkov, Relativistic quantum key distribution system with one-way quantum communication, Scientific Reports **8**, 1 (2018), 1801.02896.

[54] I. Radchenko, K. Kravtsov, S. Kulik, and S. Molotkov, Relativistic quantum cryptography, Laser Physics Letters **11**, 065203 (2014), 1403.3122.

[55] A. Datta, Quantum discord between relatively accelerated observers, Physical Review A **80**, 052304 (2009), 0905.3301.

[56] E. Jung, M.-R. Hwang, and D. Park, Quantum discord and quantum entanglement in the presence of an asymptotically flat static black hole, International Journal of Quantum Information **11**, 1350061 (2013).

[57] K. Mattle, H. Weinfurter, P. G. Kwiat, and A. Zeilinger, Dense coding in experimental quantum communication, Physical Review Letters **76**, 4656 (1996).

[58] R. Ursin, F. Tiefenbacher, T. Schmitt-Manderbach, H. Weier, T. Scheidl, M. Lindenthal, B. Blauensteiner, T. Jennewein, J. Perdigues, P. Trojek, *et al.*, Entanglement-based quantum communication over 144 km, Nature Physics **3**, 481 (2007).

[59] X.-M. Jin, J.-G. Ren, B. Yang, Z.-H. Yi, F. Zhou, X.-F. Xu, S.-K. Wang, D. Yang, Y.-F. Hu, S. Jiang, *et al.*, Experimental free-space quantum teleportation, Nature Photonics **4**, 376 (2010).

[60] S. Brito, A. Canabarro, D. Cavalcanti, and R. Chaves, Satellite-based photonic quantum networks are small-world, PRX Quantum **2**, 010304 (2021).

[61] S.-K. Liao, W.-Q. Cai, W.-Y. Liu, L. Zhang, Y. Li, J.-G. Ren, J. Yin, Q. Shen, Y. Cao, Z.-P. Li, *et al.*, Satellite-to-ground quantum key distribution, Nature **549**, 43 (2017).

[62] J. Yin, J.-G. Ren, H. Lu, Y. Cao, H.-L. Yong, Y.-P. Wu, C. Liu, S.-K. Liao, F. Zhou, Y. Jiang, *et al.*, Quantum teleportation and entanglement distribution over 100-kilometre free-space channels, Nature **488**, 185 (2012), 1205.2024.

[63] A. Villar, A. Lohrmann, X. Bai, T. Vergoossen, R. Bedington, C. Perumangatt, H. Y. Lim, T. Islam, A. Reezwana, Z. Tang, *et al.*, Entanglement demonstration on board a nano-satellite, Optica **7**, 734 (2020), 2006.14430.

[64] J. Yin, Y. Cao, Y.-H. Li, J.-G. Ren, S.-K. Liao, L. Zhang, W.-Q. Cai, W.-Y. Liu, B. Li, H. Dai, *et al.*, Satellite-to-ground entanglement-based quantum key distribution, Physical Review Letters **119**, 200501 (2017).

[65] J. Yin, Y.-H. Li, S.-K. Liao, M. Yang, Y. Cao, L. Zhang, J.-G. Ren, W.-Q. Cai, W.-Y. Liu, S.-L. Li, *et al.*, Entanglement-based secure quantum cryptography over 1,120 kilometres, Nature **582**, 501 (2020).

[66] J. Yin, Y. Cao, Y.-H. Li, S.-K. Liao, L. Zhang, J.-G. Ren, W.-Q. Cai, W.-Y. Liu, B. Li, H. Dai, *et al.*, Satellite-based

entanglement distribution over 1200 kilometers, Science **356**, 1140 (2017), 1707.01339.

[67] J. Wang, Z. Tian, J. Jing, and H. Fan, Irreversible degradation of quantum coherence under relativistic motion, Physical Review A **93**, 062105 (2016), 1601.03238.

[68] Z. Huang and H. Situ, Quantum coherence behaviors of fermionic system in non-inertial frame, Quantum Information Processing **17**, 1 (2018), 1609.02295.

[69] J. He, Z.-Y. Ding, J.-D. Shi, and T. Wu, Multipartite quantum coherence and distribution under the unruh effect, Annalen der Physik **530**, 1800167 (2018).

[70] H.-S. Zeng and H.-M. Cao, Distribution and evolution of quantum coherence for open multi-qubit systems in non-inertial frames, Annalen der Physik **533**, 2000606 (2021).

[71] S. Rana, P. Parashar, and M. Lewenstein, Trace-distance measure of coherence, Physical Review A **93**, 012110 (2016), 1511.01854.

[72] L.-H. Shao, Z. Xi, H. Fan, and Y. Li, Fidelity and trace-norm distances for quantifying coherence, Physical Review A **91**, 042120 (2015).

[73] Y.-T. Wang, J.-S. Tang, Z.-Y. Wei, S. Yu, Z.-J. Ke, X.-Y. Xu, C.-F. Li, and G.-C. Guo, Directly measuring the degree of quantum coherence using interference fringes, Physical Review Letters **118**, 020403 (2017).

[74] C. Napoli, T. R. Bromley, M. Cianciaruso, M. Piani, N. Johnston, and G. Adesso, Robustness of coherence: an operational and observable measure of quantum coherence, Physical Review Letters **116**, 150502 (2016), 1601.03781.

[75] M. Piani, M. Cianciaruso, T. R. Bromley, C. Napoli, N. Johnston, and G. Adesso, Robustness of asymmetry and coherence of quantum states, Physical Review A **93**, 042107 (2016), 1601.03782.

[76] M.-R. Hwang, D. Park, and E. Jung, Tripartite entanglement in a noninertial frame, Physical Review A **83**, 012111 (2011), 1010.6154.

[77] Sudha, A. R. U. Devi, and A. K. Rajagopal, Monogamy of quantum correlations in three-qubit pure states, Phys. Rev. A **85**, 012103 (2012).

[78] M. Plesch and V. Bužek, Entangled graphs: Bipartite entanglement in multiqubit systems, Phys. Rev. A **67**, 012322 (2003).

[79] M. Plesch and V. Bužek, Entangled graphs. ii. classical correlations in multiqubit entangled systems, Phys. Rev. A **68**, 012313 (2003).

[80] R. M. Wald, *General Relativity* (The University of Chicago Press, 1984).

[81] S.-M. Wu, Z.-C. Li, and H.-S. Zeng, Quantum coherence of multipartite w-state in a schwarzschild spacetime, EPL (Europhysics Letters) **129**, 40002 (2020).

[82] A. Dragan, J. Doukas, E. Martin-Martinez, and D. E. Bruschi, Localized projective measurement of a quantum field in non-inertial frames, Classical and Quantum Gravity **30**, 235006 (2013).

[83] T. G. Downes, I. Fuentes, and T. Ralph, Entangling moving cavities in noninertial frames, Physical review letters **106**, 210502 (2011).

[84] N. Friis, A. R. Lee, D. E. Bruschi, and J. Louko, Kinematic entanglement degradation of fermionic cavity modes, Physical Review D **85**, 025012 (2012).

[85] D. Rideout, T. Jennewein, G. Amelino-Camelia, T. F. Demarie, B. L. Higgins, A. Kempf, A. Kent, R. Laflamme, X. Ma, R. B. Mann, *et al.*, Fundamental quantum optics experiments conceivable with satellites—reaching relativistic distances and velocities, Classical and Quantum Gravity **29**, 224011 (2012).

[86] E. Martín-Martínez, I. Fuentes, and R. B. Mann, Using berry's phase to detect the unruh effect at lower accelerations, Physical Review Letters **107**, 131301 (2011).

[87] S.-M. Wu, H.-S. Zeng, and H.-M. Cao, Quantum coherence and distribution of n-partite bosonic fields in noninertial frame, Classical and Quantum Gravity **38**, 185007 (2021).